理學博士學位論文

분열성 효모에서 철 흡수 억제 전사인자 Fep1의 특성 분석

Characterization of iron uptake repressor Fep1 in *Schizosaccharomyces pombe*

2017年 2月

서울大學校 大學院

生命科學部

金 孝 鎭

Characterization of iron uptake repressor Fep1

in *Schizosaccharomyces pombe*

By

Hyo-Jin Kim

under the supervision of

Professor Jung-Hye Roe, Ph.D.

A Thesis Submitted in Partial Fulfillment

of the Requirements for the Degree of

Doctor of Philosophy

February, 2017

School of Biological Sciences

Graduate School

Seoul National University

ABSTRACT

Iron is an important cofactor for a wide variety of proteins involved in the major life processes, such as respiration and tricarboxylic acid cycle, DNA replication and repair, and nitrogen fixation. The essential redox-active property of iron that enables facile switch between ferric (Fe^{3+}) and ferrous iron (Fe^{2+}) also renders toxicity via generating reactive oxygen species. Therefore, most organisms are equipped with regulated mechanisms to maintain optimal intracellular levels of iron.

In the fission yeast *Schizosaccharomyces pombe*, two repressors Php4 and Fep1 regulate iron-dependent expression of genes for iron usage/storage and acquisition, respectively. The iron-sensing depends on the CGFS-type monothiol glutaredoxin Grx4 that binds Fe-S cluster in a homodimer or in a heterodimer with a BolA-type protein Fra2. Under iron-rich condition, Grx4 binding to Php4 causes its cytosolic sequestration, resulting in the induction of iron usage/storage genes. Grx4 also binds Fep1 regardless of iron availability. Under iron-starved condition, Grx4 and Fra2 inhibit Fep1 repressor activity, resulting in derepression of iron acquisition genes.

Fep1, a GATA-family transcription factor, binds to the promoter regions of genes for iron acquisition, such as reductive iron import (*fio1+*, *frp1+*), siderophore transport (*str1+*, *str2+*, *str3+)*, and vacuolar transport (*abc3+*), to avoid iron overload under iron-rich conditions. The N-terminal DNA-binding domain of Fep1 contains four conserved cysteines located between the two zinc finger motifs. It has been demonstrated that the N-terminal 241 aa residues of Fep1 can bind to the target promoters *in vivo* under iron-replete condition. Through this N-terminal

domain, Fep1 is known to interact with the monothiol glutaredoxin domain of Grx4 under iron-starved condition. Under iron-starved condition, Fep1 is released from binding to its target sites, inducing iron uptake genes. Fep1 orthologs are well conserved, especially in the DNA binding domain, across filamentous fungi, such as *Ustilago maydis* (Urbs1), *Neurospora crassa* (SRE), *Histoplasma capsulatum* (Sre1), *Aspergillus spp.* (SREA), *Candida albicans* (Sfu1), and *Cryptococcus neoformans* (Cir1).

Even though the function and interaction partners of Fep1 have been elucidated extensively in *S. pombe*, the molecular basis by which Fep1 is inactivated under iron starvation remains unknown. In this study, to elucidate the mechanism behind iron-sensing by Fep1, I pursued biochemical and spectroscopic analyses of Fep1, in full length and truncated forms, as isolated or reconstituted proteins, with the wild type or substituted cysteine mutations. Evidences are presented that Fep1 binds iron, in the form of Fe-S cluster. Spectroscopic and biochemical analyses of as isolated and reconstituted Fep1 suggest that the dimeric Fep1 binds Fe-S clusters. Iron to acid-labile sulfide stoichiometry of purified Fep1-N238 was roughly 1 : 1 in both before and after chemical reconstitution. Furthermore, the reconstitution of the His-tagged Fep1-N238 requires not only iron donor but also sulfide donor, indicating that Fep1 binds [Fe-S] clusters. The mutation study revealed that the cluster-binding depended on the conserved cysteines located between the two zinc fingers in the DNA binding domain. EPR analyses revealed [Fe-S]-specific peaks indicative of mixed presence of [2Fe-2S], [3Fe-4S], or [4Fe-4S]. Overall, the finding that Fep1 is an Fe-S protein fits nicely with the model that the Fe-S-trafficking Grx4 senses intracellular iron environment and modulates the activity of Fep1.

Key Words

; Monothiol glutaredoxin, Iron homeostasis, Fe-S cluster, Fep1, EPR

CONTENTS

LIST OF FIGURES

LIST OF TABLES

LIST OF ABBREVIATIONS

EPR	Electron Paramagnetic Resonance
BiFC	Bimolecular flouorescence complementation
DTT	dithiothreitol
DNA	deoxyribocunleic acid
SDS	sodium dodecyl sulfate
EDTA	ethylenediamine tetraacetate
EtBr	ethidium bromide
GFP	green fluorescence protein
IPTG	isopropyl-β-D-thiogalactopyranoside
Kb	kilo base pair
kDa	kilo Dalton
OD	optical density
ORF	open reading frame
PAGE	polyacrylamide gel electrophoresis
PCR	polymerase chain reaction
WT	wild-type
Grx	glutaredoxin
Trx	thioredoxin
GSH	reduced glutathione, γ-L-glutamyl-L-cysteinylglycin

CHAPTER I.

INTRODUCTION

I.1. Iron homeostasis and disease

Iron is an important cofactor for a wide variety of proteins involved in the major life processes, such as respiration, tricarboxylic acid cycle, DNA replication and repair, and nitrogen fixation (Kaplan & Ward, 2013). In high concentrations, however, the essential redox-active property of iron that enables facile switch between ferric (Fe^{3+}) and ferrous iron (Fe^{2+}) also renders toxicity via generating reactive oxygen species. Therefore, most organisms are equipped with regulated mechanisms to maintain optimal intracellular levels of iron. Because of the low bioavailability of iron, iron deficiency is the most common and widespread nutritional disorder in the world (Zimmermann & Hurrell, 2007). At the other extreme, iron overload diseases are common systemic iron disorders primarily caused by mutations in proteins that sense, regulate, or mediate iron absorption from the gastrointestinal tract (Fleming & Ponka, 2012, Nairz & Weiss, 2006). Increased iron absorption and storage leads to excessive iron accumulation in various organs (mainly liver, heart, and pancreas) causing progressive organ damage and increased mortality as a consequence of elevated oxidative stress. In addition to systemic iron disorders, numerous human diseases have also been linked with iron dysregulation at the cellular level. For example, specific defects in Fe-S cluster biogenesis factors lead to Friedreich's ataxia, X-linked sideroblastic anemia, sideroblastic-like microcytic anemia, and myopathy (Sheftel, Stehling et al., 2010, Ye & Rouault, 2010).

The fungi *Saccharomyces cerevisiae* and *Schizosaccharomyces pombe* have proven to be effective models for studying eukaryotic iron homeostasis at the cellular level. Despite their relative simplicity, biochemical and genetic studies in yeast have been critical for identifying proteins required for iron uptake, intracellular iron transport and mobilization, and heme and Fe-S cluster biogenesis in higher eukaryotes (Askwith & Kaplan, 1998, De Freitas, Wintz et al., 2003, Lill &

Muhlenhoff, 2008, Wingert, Galloway et al., 2005). Furthermore, genome-wide studies in yeast have revealed how eukaryotic cells adapt to both iron deficiency (Philpott, Leidgens et al., 2012) and iron overload (Jo, Loguinov et al., 2008, Lin, Li et al., 2011). In addition, yeast studies have been pivotal in defining the pathophysiology of human diseases of iron metabolism, such as Friedreich's ataxia and aceruloplasminemia (Bleackley & Macgillivray, 2011, Lodi, Tonon et al., 2006, Pandolfo & Pastore, 2009, Rouault & Tong, 2008).

I.2. Regulation of iron homeostasis in *Schizosaccaromyces pombe*

I.2.1. Fep1, the iron-regulatory GATA-type repressor

In the fission yeast *S. pombe*, two repressors Php4 and Fep1 regulate iron-dependent expression of genes for iron usage/storage and acquisition, respectively (Brault, Mourer et al., 2015, Labbe, Khan et al., 2013, Mercier, Pelletier et al., 2006, Pelletier, Beaudoin et al., 2003). Fep1, a GATA-family transcription factor, binds to the promoter regions of genes for iron acquisition, such as reductive iron import (*fio1+, frp1+*), siderophore transport (*str1+, str2+, str3+),* and vacuolar transport (*abc3+*), to avoid iron overload under iron-rich conditions (Fig I-1). The N-terminal DNA-binding domain of Fep1 contains four conserved cysteines located between the two zinc finger motifs (Brault et al., 2015, Labbe et al., 2013). It has been demonstrated that the N-terminal 241 aa residues of Fep1 can bind to the target promoters *in vivo* under iron-replete condition (Jbel, Mercier et al., 2009). Through this N-terminal domain, Fep1 is known to interact with the monothiol glutaredoxin domain of Grx4 under iron-starved condition (Jbel, Mercier et al., 2011). Repression by DNA-bound Fep1 requires recruitment and binding of the co-repressors Tup11 and Tup12 in an iron-independent manner, and deletion mapping studies have delineated the Tup11 interaction domain in the

Fig I-1. Models for the regulatory action of iron-responsive transcription factors in response to levels of iron (Brault, A et al., 2015)

A. In *S. pombe*, Fep1 interacts with GATA elements in promoters of *php4*$^+$ and iron transport genes. Fep1 represses target gene transcription with the help of the corepressor Tup11 or Tup12. In this context, Fra2 may participate in the dissociation of the GRX domain (of Grx4) from the N-terminal portion of Fep1 by forming a [2Fe-2S] (red circle) Fra2-GRX domain heterodimer, allowing the N-terminus of Fep1 to be free and available for binding to chromatin and repressing transcription. Under conditions of iron excess (Fe+), Grx4 acquires an [2Fe-2S] cluster that would in turn trigger the interaction between the GRX domain (of Grx4) and the C-terminal region of Php4. This interaction between the GRX domain and Php4 would disrupt the Php4/Php2/Php3/Php5 heteromeric complex, leading to Php4 release and inactivation. The Grx4-mediated inactivation of Php4 would lead to its recruitment by the exportin Crm1 and then to its subsequent export from the nucleus to the cytoplasm. The absence of Php4 enables fep1$^+$ and iron utilization genes to be expressed through the CCAAT-binding core complex that is composed of Php2, Php3, and Php5.

B. Grx4 and Fra2 are inhibitory partners of Fep1, blocking its association with chromatin and preventing its repressive effect on target gene expression. In the absence of iron (Fe-), Php4 forms a complex with Php2, Php3, Php5, and Grx4. Because only the TRX domain of Grx4 interacts with Php4, this leaves the repression domain of Php4 available to repress several genes, including fep1$^+$ and several others encoding iron-using proteins. Php4 nuclear import is mediated by distinct karyopherins, namely Imp1, Cut15, and Sal3.

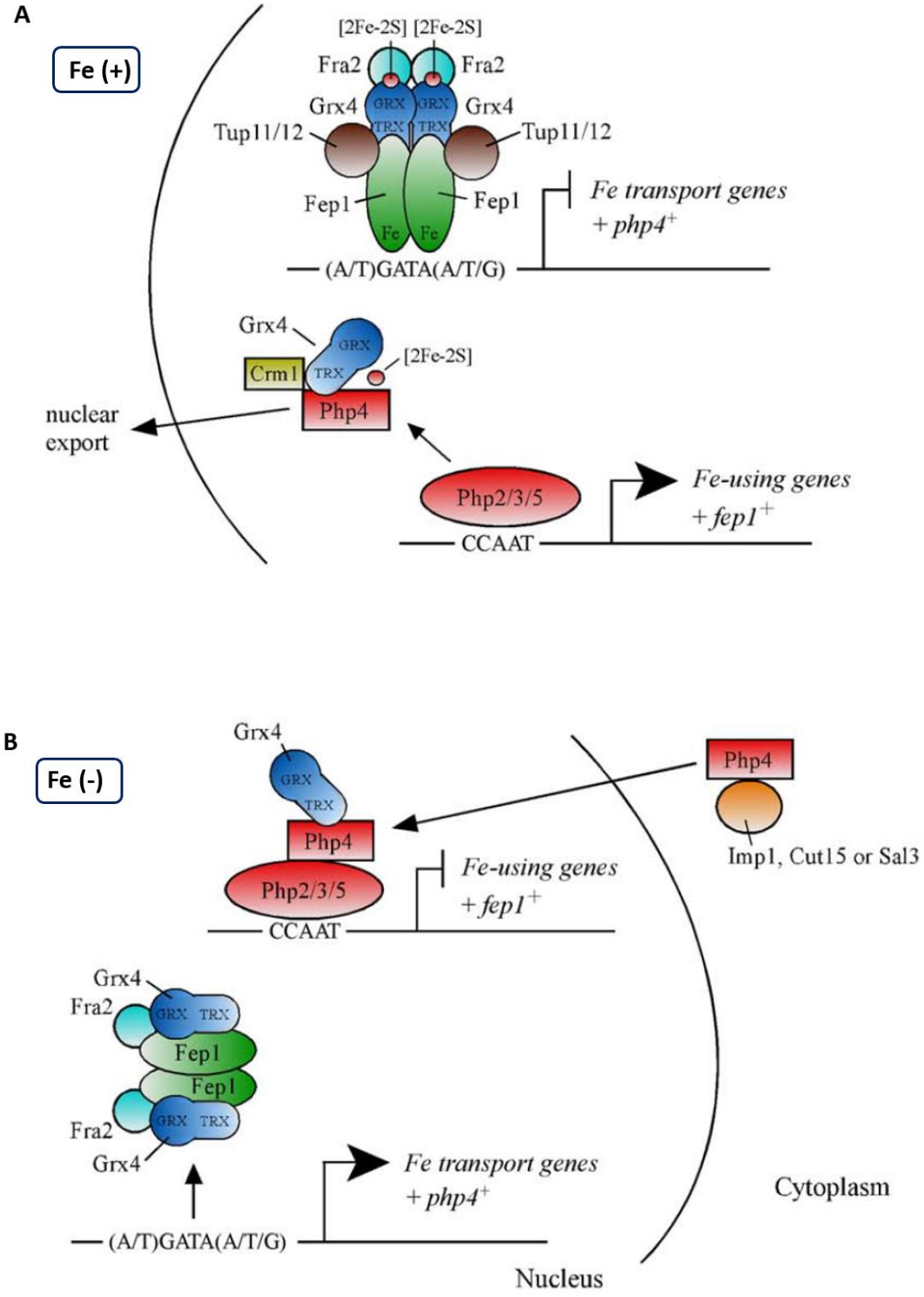
A
Fe (+)
[2Fe-2S] [2Fe-2S]
Fra2
Fra2
Grx4
GRX
GRX
Grx4
TRX
TRX
Tup11/12
Tup11/12
Fep1
Fep1
Fe
Fe
Fe transport genes
+ php4+
(A/T)GATA(A/T/G)
Grx4
GRX
Crm1
TRX
[2Fe-2S]
Php4
nuclear
export
Php2/3/5
Fe-using genes
+ fep1+
CCAAT
B
Fe (-)
Grx4
GRX
TRX
Php4
Php2/3/5
Fe-using genes
+ fep1+
CCAAT
Php4
Imp1, Cut15 or Sal3
Grx4
Fra2
GRX TRX
Fep1
Fep1
GRX TRX
Fra2
Grx4
Fe transport genes
+ php4+
(A/T)GATA(A/T/G)
Cytoplasm
Nucleus

C-terminus of Fep1 (Fig I-2) (Znaidi, Pelletier et al., 2004). The C-terminus of Fep1 also contains a dimerization domain that is required for efficient repression of Fep1 target genes (Pelletier, Trott et al., 2005). Under iron-starved condition, Fep1 is released from binding to its target sites, inducing iron uptake genes (Jbel et al., 2009). Fep1 orthologs are well conserved (Fig I-2), especially in the DNA binding domain, across filamentous fungi, such as *Ustilago maydis* (Urbs1) (An, Mei et al., 1997), *Neurospora crassa* (SRE) (Zhou, Haas et al., 1998), *Histoplasma capsulatum* (Sre1) (Chao, Marletta et al., 2008), *Aspergillus spp.* (SREA) (Haas, Zadra et al., 1999, Schrettl, Kim et al., 2008), *Candida albicans* (Sfu1)(Lan, Rodarte et al., 2004), and *Cryptococcus neoformans* (Cir1) (Jung, Sham et al., 2006).

I.2.2. Php4, a key regulator for iron economy

The transcriptional repressor Php4 also controls iron homeostasis in *S. pombe* by regulating expression of genes involved in iron-dependent metabolic pathways. Php4 binds to a heterotrimeric protein complex composed of Php2, Php3, and Php5. Under iron replete conditions, Php4 is not expressed and the Php2/Php3/Php5 complex activates expression of its target genes by binding to CCAAT sequences in their promoters (Fig I-1A). Php2/Php3/Php5-regulated genes encode proteins involved in iron-dependent metabolic pathways such as iron-sulfur cluster biogenesis, heme biosynthesis, the mitochondrial electron transport chain, and the tricarboxylic acid cycle (Mercier et al., 2006). Under low iron conditions, Php4 is expressed and binds to the Php2/Php3/Php5 complex, causing it to switch from an activator to a repressor (Fig I-1B). Thus, iron-utilizing pathways are downregulated as an iron sparing response to lower bioavailable iron.

Php4 itself is regulated at the transcriptional level by Fep1 since the php4+ gene contains GATA elements within its promoter (Mercier et al., 2006). When iron

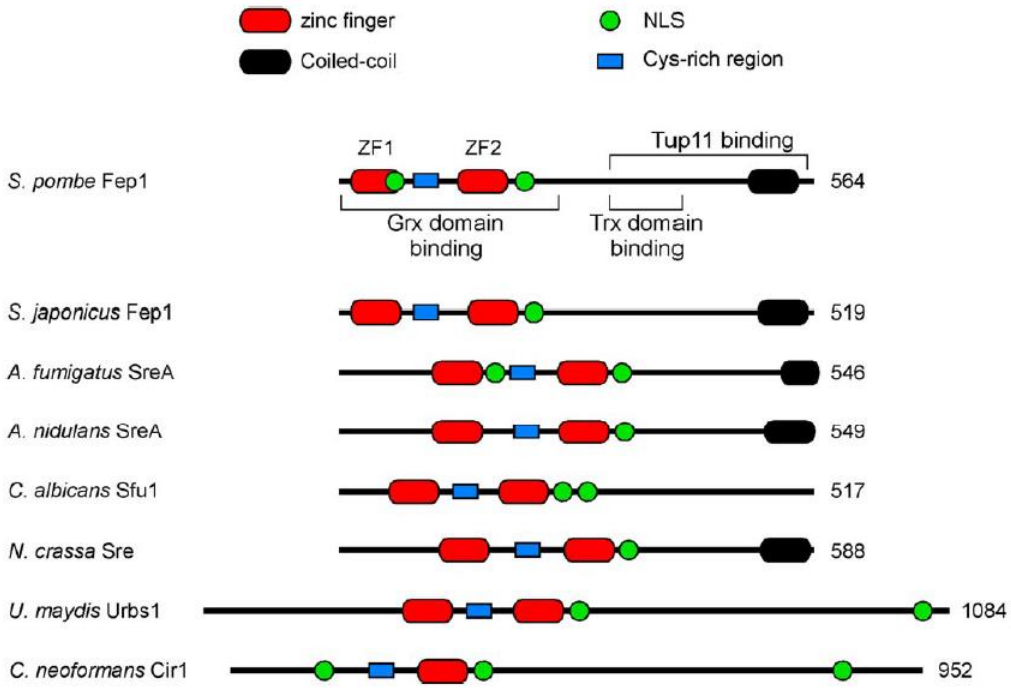

Fig I-2. Domain comparisons of GATA-type iron regulatory transcription factors (Brault, A et al., 2015).

ZF1 and ZF2 (red) are the N-terminal and C-terminal GATA-type zinc finger motifs, respectively. Four highly conserved Cys residues, denoted Cys-rich region (blue). A conserved coiled-coil region (black). Putative NLSs are indicated in green. Regions of Fep1 that interact with the GRX and TRX domains of Grx4 as well as with the corepressor Tup11 are indicated within brackets.

levels are high, Fep1 binds to the promoter of php4+ and represses the transcription of php4+ (Fig I-1A). When iron levels are low, Fep1 is unable to inhibit php4+ transcription and Php4 is subsequently expressed, allowing it to repress iron-utilizing pathways via the Php2/Php3/Php5 complex (Fig I-1B). A genome-wide DNA microarray study also revealed that the fep1+ gene contains CCAAT cis-acting elements in its promoter region and is downregulated in a Php4-dependent manner in response to iron deprivation (Fig I-1B) (Mercier, Watt et al., 2008). This reciprocal regulatory loop between two iron-responsive repressors through mutual control of each other's expression allows direct crosstalk between iron acquisition and iron utilization pathways to fine tune iron homeostasis in *S. pombe*.

I.2.3. Roles for Grx4 in iron homeostasis in *S. pombe*

The activities of both Fep1 and Php4 are controlled at the post-translational level by *S. pombe* Grx4, a member of the multidomain CGFS Grx subfamily. Grx4 is required to regulate the activity of both Fep1 and Php4 through specific protein-protein interactions.

Fep1 is regulated through Grx4 at the post-translational level (Jbel et al., 2011, Kim, Kim et al., 2011). Grx4 was shown to constitutively interact with Fep1; however, the Fep1-Grx4 complex resides in the nucleus regardless of iron status inside the cell. Under iron-starved condition, Grx4 and Fra2 inhibit Fep1 repressor activity, resulting in derepression of iron acquisition genes. When iron is abundant, Grx4 is unable to inhibit Fep1 repressor function, although it still physically interacts with Fep1 (Fig I-1A) (Jbel et al., 2011, Kim et al., 2011).

Deletion of grx4 leads to constitutive repression of both Php4- and Fep1-regulated genes and constitutive nuclear localization of Php4 (Fig I-3) (Jbel et al., 2011, Kim et al., 2011, Mercier & Labbe, 2009). Yeast two-hybrid and bimolecular

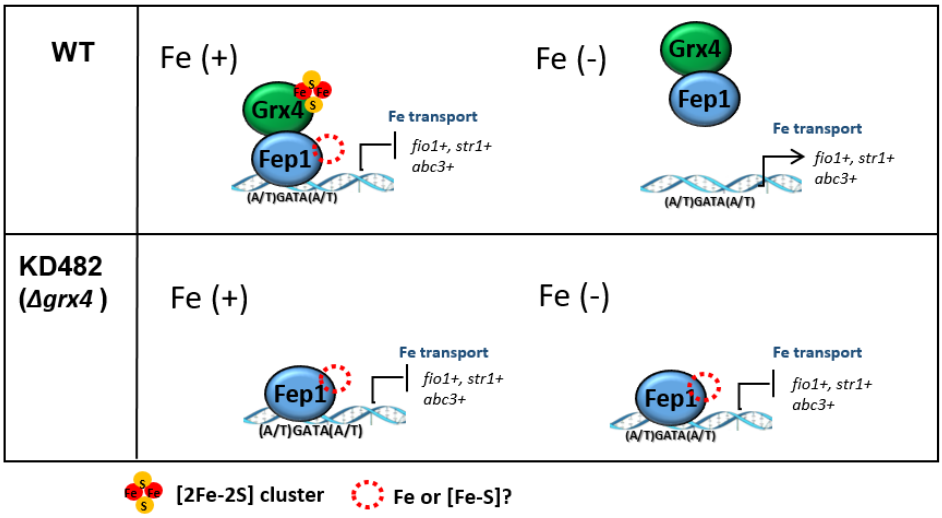

Fig I-3. A schematic model of iron-dependent regulation of Fep1 repressor activity.

[Fe-S]-binding Grx4-Fra2 has been reported to bind Fep1. In the presence of sufficient iron, Fep1 represses genes for iron acquisition. Under iron starvation, Fep1 repressor activity is inhibited by Grx4 and Fra2, de-repressing iron acquisition genes. Whether iron binds to Fep1 as a mononuclear form or as an Fe-S cluster is under question.

fluorescence complementation experiments established that Grx4 physically interacts with Php4 regardless of cellular iron levels. However, under iron-replete conditions Grx4 promotes Php4 export to the cytosol by facilitating direct interaction with the nuclear exportin Crm1 (Fig I-1A).

I.3. CGFS monothiol glutaredoxins

Glutaredoxins (Grxs) were initially identified as members of the thioredoxin (Trx)-fold family that catalyze thiol-disulfide exchange reactions in a glutathione (GSH)-dependent manner via a conserved CPY/FC active site (Lillig, Berndt et al., 2008). Classical dithiol Grxs that utilize a dithiol mechanism to reduce intramolecular disulfide bonds require both cysteines for catalytic activity, while Grxs that catalyze glutathionylation/deglutathionylation reactions via a monothiol mechanism require only the N-terminal active site Cys (Fernandes & Holmgren, 2004). With the increasing number of sequenced genomes, several Grxs with divergent active site sequences have been identified, thus requiring an updated phylogenetic classification for the Grx family (Couturier, Jacquot et al., 2009). The most widespread Grxs present in both prokaryotes and eukaryotes are grouped in Class I, which includes the classical dithiol Grxs, and in Class II, which are defined as monothiol Grxs with a conserved CGFS active site. CGFS-type monothiol Grxs can be further classified into two groups: single domain CGFS Grxs and multidomain CGFS Grxs with an N-terminal Trx-like domain and one or more Grx-like domains (Fig I-4).

Unlike Class I Grxs, CGFS Grxs have little or no thiol-disulfide oxidoreductase activity when tested with standard Grx model substrates (Fernandes, Fladvad et al., 2005, Ken, Chen et al., 2011, Mesecke, Mittler et al., 2008, Tamarit, Belli et al., 2003, Zaffagnini, Michelet et al., 2008). However, the CGFS active site is required

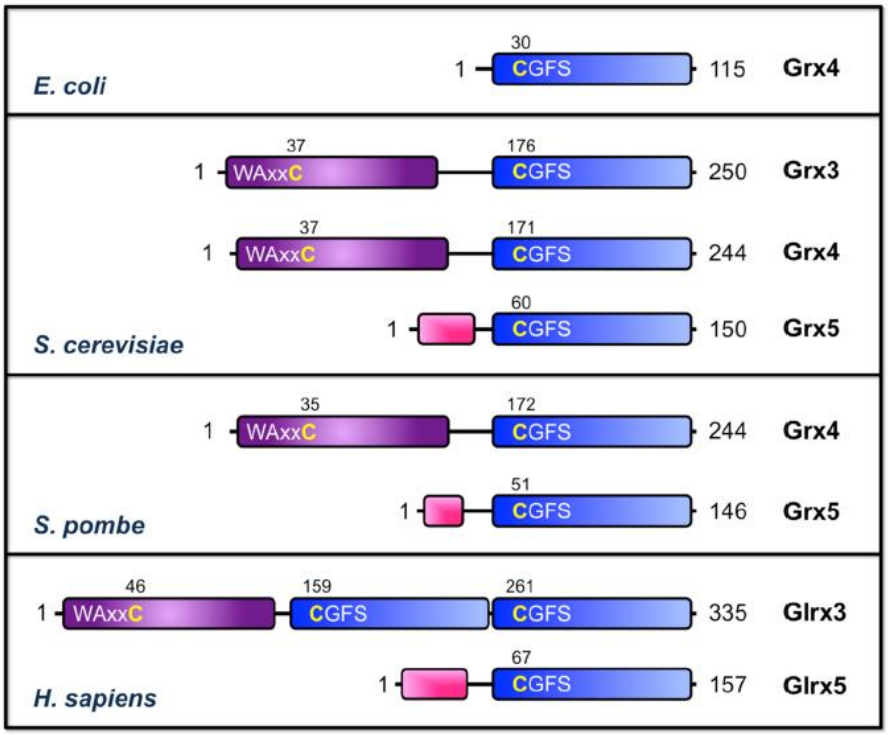

Fig I-4. Domain structure of CGFS monothiol Grxs from *E. coli, S. cerevisiae, S. pombe,* and *H. sapiens* (Li, H et al., 2012)

The Trx-like domains and Grx-like domains are shown as purple and blue boxes, respectively. The conserved cysteines in the active sites of the Trx and Grx domains are numbered and shown in yellow. Predicted or known mitochondrial targeting signals are shown as pink boxes.

for a different purpose: coordination of a [2Fe-2S] cluster. Both single and multidomain CGFS Grxs form $[2Fe\text{-}2S]^{2+}$-bridged homodimers with all-cysteinyl ligation provided by the two CGFS active sites and two GSH molecules (Bandyopadhyay, Gama et al., 2008, Haunhorst, Berndt et al., 2010, Iwema, Picciocchi et al., 2009, Li, Mapolelo et al., 2009, Picciocchi, Saguez et al., 2007, Ye, Jeong et al., 2010, Yeung, Gold et al., 2011). Formation of this Fe-S complex is supported by studies in *S. cerevisiae* demonstrating that iron binding to CGFS Grxs *in vivo* requires the CGFS motif, sufficient cellular GSH levels, and the mitochondrial Fe-S assembly machinery (Muhlenhoff, Molik et al., 2010). The first crystal structure of a [2Fe-2S]-bridged CGFS Grx homodimer was published for *E. coli* Grx4 in 2009, confirming that two GSH molecules are covalently linked to the cluster, but held in place by non-covalent interactions with the GSH binding pocket of each Grx4 monomer (Iwema et al., 2009). There is currently no published crystal structure available for a [2Fe-2S]-bound multidomain CGFS Grx, thus the orientation of the Trx-like domain in relation to the [2Fe-2S]-bridged Grx-like domain(s) is unknown.

In eukaryotes, single domain CGFS Grxs (e.g., yeast Grx5 and human Glrx5, see Fig I-4) are localized to mitochondria or chloroplasts and have been implicated in the maturation of Fe-S cluster proteins (Herrero, Belli et al., 2010, Rouhier, Couturier et al., 2010, Ye & Rouault, 2010). In contrast, multidomain CGFS Grxs (e.g., yeast Grx3/4 and human Glrx3) display cytosolic/nuclear localization where they are proposed to play dual roles in cytosolic iron trafficking and iron regulation (Jbel et al., 2011, Kumanovics, Chen et al., 2008, Muhlenhoff et al., 2010, Ojeda, Keller et al., 2006, Pujol-Carrion, Belli et al., 2006). The Fe-S biogenesis function of single domain CGFS Grxs as well as the trafficking and regulatory functions of multidomain CGFS Grxs in yeast are all dependent on the presence of the conserved Cys in the CGFS active site, suggesting that coordination of the [2Fe-2S] cluster is essential to these functions (Belli, Polaina et al., 2002, Jbel et al., 2011,

Kim et al., 2011, Molina, Belli et al., 2004, Muhlenhoff et al., 2010, Ojeda et al., 2006)

I.3.1. Mitochondrial monodomain Grxs in the maturation of Fe-S protein

A role for yeast mitochondrial Grx5p in Fe–S cluster biogenesis was initially suggested by studies in a grx5 deletion mutant. These yeast cells displayed deficient cluster assembly for at least two Fe–S proteins (aconitase and succinate dehydrogenase), leading to impaired respiratory growth and increased sensitivity to oxidative stress as a result of the accumulation of free iron in the cell (Rodriguez-Manzaneque, Ros et al., 1999, Rodriguez-Manzaneque, Tamarit et al., 2002). Later, radio-labelled ^{55}Fe immunoprecipitation experiments revealed that Grx5p most likely facilitates the transfer of preassembled clusters from U-type ISC scaffold proteins (Isu1p) to acceptor proteins and bioinformatics predictions indicated that it is involved either in regulating the Nfs1p cysteine desulfurase or in the assembly of Fe–S clusters on scaffold proteins (Alves, Herrero et al., 2004, Muhlenhoff, Gerber et al., 2003). The specific interaction of Grx5p with the A-type ISC scaffold protein Isa1p, but not Isa2p, demonstrated by yeast two hybrid experiments, further supports the view that Grxs participate in the initial steps of cluster assembly or in the transfer of preassembled clusters (Vilella, Alves et al., 2004). Furthermore, complementation experiments of the yeast grx5 deletion strain demonstrated that most CGFS Grxs from prokaryotic or eukaryotic sources other than yeast, when targeted to the yeast mitochondrial matrix, can functionally substitute for Grx5p, suggesting that this role might be conserved throughout evolution (Bandyopadhyay et al., 2008, Molina-Navarro, Casas et al., 2006).

A series of recent papers indicates that the recombinant versions of bacterial, human, yeast and plant Grx5 orthologues produced in *E. coli* are able to incorporate labile Fe–S clusters (Bandyopadhyay et al., 2008, Picciocchi et al., 2007). Owing to their labile nature and to technical limitations, the presence of Fe–S clusters complexed to these CGFS Grxs has yet to be confirmed *in vivo*. Analytical

and spectroscopic [UV-visible absorption/circular dichroism (CD), resonance Raman and Mössbauer] analyses of anaerobically purified proteins or proteins repurified after *in vitro* cysteine desulfurase-mediated cluster reconstitution of apoproteins indicated that two plant CGFS Grxs (the plastid GrxS14 and GrxS16) could incorporate one $[2Fe–2S]^{2+}$ cluster per homodimer with complete cysteinyl ligation (Bandyopadhyay et al., 2008). Cysteine mutagenesis studies of these Grxs, the requirement for GSH in GrxS14 reconstitution experiments and the recent determination of the 3D structure of the *E. coli* Grx4 holodimer revealed that the [2Fe–2S] cluster is ligated by the active-site cysteines of two Grx monomers and two GSH molecules (Bandyopadhyay et al., 2008, Iwema et al., 2009, Rouhier, Unno et al., 2007). The $[2Fe–2S]^{2+}$ clusters of these CGFS Grxs are oxidatively and reductively labile, as evidenced by cluster degradation on exposure to air and following anaerobic reduction with dithionite (Bandyopadhyay et al., 2008).

I.3.2. Nucleo-cytosolic multidomain Grxs in iron metabolism

Most multidomain class II Grxs are localized in the cytosol and/or in the nucleus (Babichev & Isakov, 2001, Cheng, Liu et al., 2011, Lopreiato, Facchin et al., 2004, Molina et al., 2004). Although not involved in Fe–S cluster binding, the N-terminal Trx-domain found in these proteins proved to have important contributions. Despite the lack of specific NLS signature, the Trx-domain is responsible for the nuclear localization of yeast Grx3/4 (Molina et al., 2004). Moreover, it is essential for their roles in iron trafficking and Aft1 regulation in vivo, possibly functioning as a docking site facilitating the interaction with partner proteins (Hoffmann, Uzarska et al., 2011, Li et al., 2009). Accordingly, its importance was also confirmed for the interactions of Grx4 with Fep1 and Php4, two transcriptional regulators of iron homeostasis in *S. pombe* (Jbel et al., 2011, Vachon, Mercier et al., 2012) and for the demonstrated role in actin cytoskeleton organization (Pujol-Carrion & de la Torre-Ruiz, 2010). Interestingly, all these functions do not require the remnant

cysteine of the Trx-like active site signature (Hoffmann et al., 2011, Pujol-Carrion & de la Torre-Ruiz, 2010).

Most multidomain Grxs tested so far (ScGrx3, ScGrx4, SpGrx5 poplar and Arabidopsis GrxS17 and human Grx3) are able to restore the deficiency of yeast grx5 mutant when they are expressed in mitochondria (Bandyopadhyay et al., 2008, Cheng, Zhang et al., 2011, Li et al., 2009), (Kim et al., unpublished data). These data suggested that these Grxs could fulfill a carrier function similar to Grx5 isoforms, i.e., to accept an Fe–S cluster from a donor and to transfer it to an acceptor.

Besides their involvement in Aft1/2-dependent iron sensing (detailed below), an independent function in the regulation of intracellular Fe trafficking was suggested (Fig I-5). Indeed, the deletion of both Grx3 and 4 is lethal (Muhlenhoff et al., 2010). Using a conditional mutant strain, it was shown that all iron-requiring reactions in cytosol, mitochondria and nucleus are affected. Despite the induction of Aft1-dependent iron uptake, the Grx3 and 4 depletion also leads to the impairment of several mitochondrial iron-dependent proteins such as complexes II and III, the mitochondrial Fe–S protein aconitase, but also of cytosolic proteins such as the heme-containing catalase (Muhlenhoff et al., 2010). In addition, the activity of several proteins containing di-iron centers such as the cytosolic ribonucleotide reductase (RNR), the mitochondrial mono-oxygenase Coq7 are also strongly decreased (Muhlenhoff et al., 2010, Zhang, Liu et al., 2011). These Grx3/4 depleted cells also displayed a decreased iron level in mitochondria and an increased iron level in the cytosol respectively.

Altogether, these data indicate that, in *S. cerevisiae*, Grx3 and 4 facilitate the correct assembly of several types of iron containing centers in various proteins. The exact biochemical role of these Grxs is however unclear. Since the mutation of the active site cysteine abolished the ability of these Grxs to function in iron regulation and trafficking, the role might be either related to their ability to bind an Fe–S cluster, which was proved to occur *in vivo* or to its inability to mediate

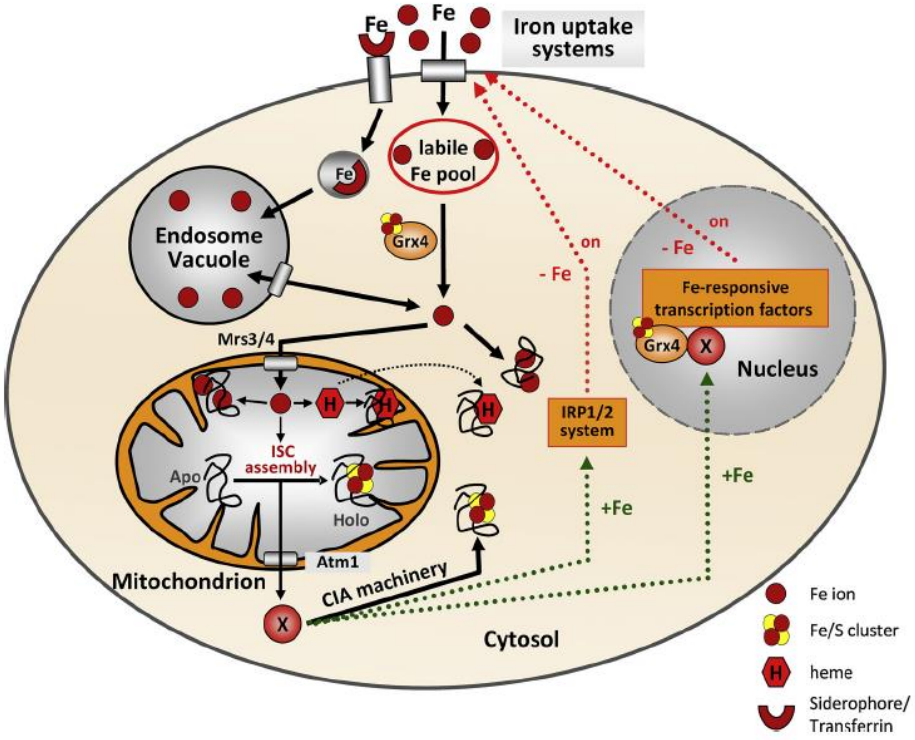
Fe
Fe
Iron uptake systems
labile Fe pool
Fe
Endosome Vacuole
Grx4
on
- Fe
on
- Fe
Fe-responsive transcription factors
Grx4
X
Nucleus
Mrs3/4
H
H
H
IRP1/2 system
ISC assembly
Apo
Holo
+Fe
+Fe
Atm1
Mitochondrion
CIA machinery
X
Cytosol
Fe ion
Fe/S cluster
heme
Siderophore/ Transferrin

Fig I-5. Intracellular iron trafficking and the regulation of cellular iron uptake in eukaryotes (Muhlenhoff, U. et al., 2015).

Iron ions acquired at the plasma membrane by high- and low-affinity iron uptake systems enter the cytosol, where they likely bind to diverse low molecular weight biological ligands, forming the labile iron pool. In parallel, fungi internalize iron siderophore complexes and vertebrates internalize iron bound to transferrin by receptor mediated endocytosis. Internalized iron is released in the endosomal/vacuolar compartment from where it is exported into the cytosol by the high affinity iron transporter Fth1/Fet5 and Smf3 (vertebrate DMT1) (Philpott, 2006). Cytosolic iron is transported into the mitochondrial matrix by the mitochondrial carrier family proteins Mrs3/4 (vertebrate MFRN1 and 2) where it is used for heme synthesis and the de novo synthesis of Fe/S clusters which is catalyzed by the mitochondrial ISC assembly system (Lill et al., 2012). In fungi, excess cytosolic iron is exported into the vacuole by the vacuolar divalent metal transporter Ccc1. In vertebrates, iron is stored in ferritin in the cytosol. The essential cytosolic monothiol glutaredoxin Grx4 (mammalian PICOT) plays acentral role in cytosolic iron trafficking. Grx4 accepts iron from the cytosolic labile iron pool in form of an Fe/S cluster and is crucially involved in the donation of iron to cytosolic iron-dependent enzymes and the cytosolic iron sulfur protein assembly (CIA) system (Paul and Lill, 2015). The latter further requires an unknown sulfur-containing low-molecular weight solute (X) that is produced by the mitochondrial ISC system and exported into the cytosol by the mitochondrial inner membrane ABC transporterAtm1 (vertebrate ABCB7) (Lill et al., 2014a). Cellular iron acquisition is tightly regulated. In vertebrates, the cytosolic iron regulatory proteins IRP1 and IRP2 play key roles in the posttranscriptional regulation of iron metabolism. Both bind to iron-responsive elements (IREs) of iron-regulated mRNAs. Under high iron conditions, the CIA system assembles a [4Fe-4S] cluster on IRP1 which transforms IRP1 into a cytosolic aconitase that no longer binds to IREs (Fig. 3). In fungi, genes involved in iron uptake at theplasma membrane are controlled by iron-responsive transcriptional regulators that respond to two iron-dependent intracellular signals: (1) A Grx4 bound Fe/S-cluster that functions as sensor for the status of the cytosolic iron pool. (2) A key regulatory molecule (X) that signals the iron status of the mitochondrial ISC systems.

GSH-dependent reactions (Hoffmann et al., 2011, Muhlenhoff et al., 2010).

I.4. CGFS monothiol glutaredoxins and BolA proteins

I.4.1. Evolutive conservation of the Grx-BolA interaction

There are a lot of evidences that the class II Fe–S Grx–BolA functional relationship is conserved in both prokaryotes and eukaryotes. Indeed, both genes are found in adjacent position in several prokaryote genomes and a strong co-occurrence exists between both genes (Couturier et al., 2009, Huynen, Spronk et al., 2005). Moreover, hybrid proteins where a BolA domain is fused to a Grx domain are present in some proteobacteria of the Methylococcale order. Besides these genomic evidences, highthroughput approaches experimentally confirmed a physical interaction for *S. cerevisiae, Drosophila melanogaster*, *E. coli* and *A. thaliana* proteins (Arabidopsis Interactome Mapping, 2011, Butland, Babu et al., 2008, Giot, Bader et al., 2003, Ho, Gruhler et al., 2002, Ito, Tashiro et al., 2000, Krogan, Cagney et al., 2006).

During the last five years, the Grx–BolA interaction has been more extensively studied using targeted biochemical and cellular approaches, focusing in particular on the molecular and structural determinants involved in the formation of Grx–BolA holo-heterodimer (Couturier, Wu et al., 2014, Kumanovics et al., 2008, Li et al., 2009). However, despite the demonstration that proteins from *E. coli*, human and *A. thaliana* can form [2Fe–2S] cluster-bridged heterodimer (Fig I-6) (Dhalleine, Rouhier et al., 2014, Li, Mapolelo et al., 2012, Yeung et al., 2011), their involvement in the regulation of iron homeostasis has been demonstrated only in *S. cerevisiae* and *S. pombe*.

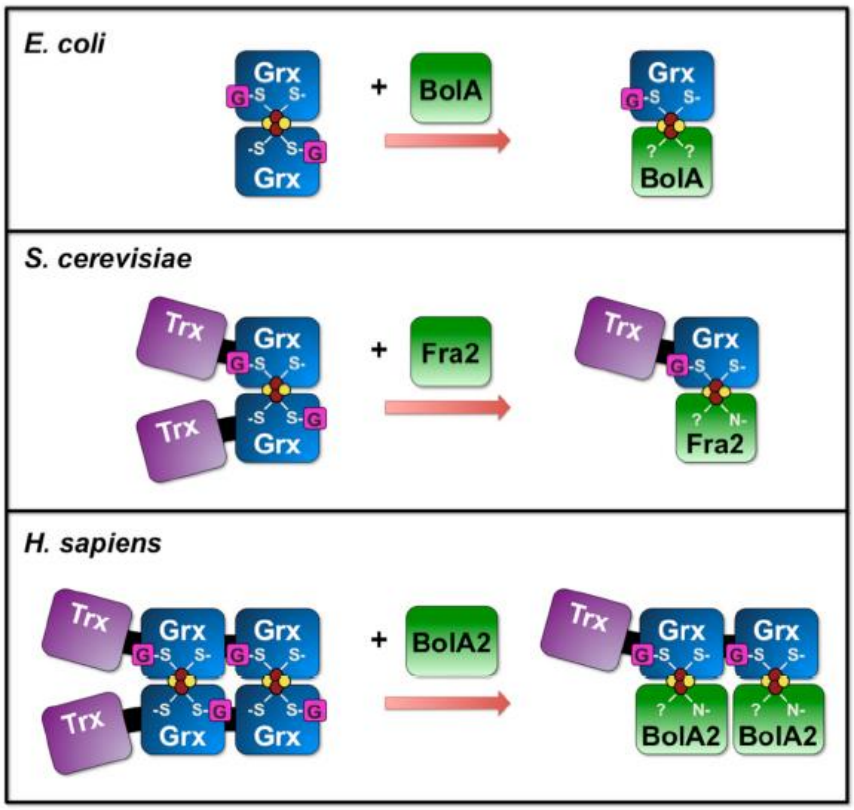

Fig I-6. Models for [2Fe-2S] Grx homodimers (left) and [2Fe–2S]$^{2+}$ Grx-BolA heterocomplexes (right) characterized from *E. coli*, *S. cerevisiae*, and *H. sapiens* (Li, H et al., 2012).

In each case, Grx-BolA heterocomplexes can be formed by titration of Grx homodimers with the apo BolA-like protein. In all CGFS Grx homodimers, the active site cysteines in the Grx-like domains and 2 GSH molecules ligate the [2Fe-2S] clusters. For yeast and human Grx-BolA heterocomplexes, each [2Fe-2S] cluster is ligated by one Grx domain active site cysteine, one GSH, a histidine from the BolA-like protein and an unidentified 4th ligand. For the *E. coli* [2Fe-2S] Grx4-BolA heterodimer, the ligands provided by BolA have not been identified.

I.4.2. Roles of Grx3/4 and Fra2 in iron homeostasis in *S. cerevisiae*

In *S. cerevisiae*, the iron metabolism is controlled at the transcriptional level by two major transcription factors, Aft1/2 constituting the sensing system under low-iron conditions. Aft1 and its paralog Aft2 are involved in the response to iron deficiency by activating the iron regulon i.e., genes coding for proteins involved in iron uptake and intracellular sequestration and in mitochondrial iron metabolism.

Iron-dependent inhibition of both Aft1 and Aft2 activity is regulated by a cytosolic signaling pathway comprised of the Cys-Gly-Phe-Ser (CGFS) monothiol glutaredoxins Grx3 and Grx4, the BolA-like protein Fe repressor of activation-2 (Fra2), and the aminopeptidase P-like protein Fe repressor of activation-1 (Fra1), which relays an inhibitory signal that is dependent on the synthesis of mitochondrial Fe-S clusters (Kumanovics et al., 2008, Ojeda et al., 2006, Pujol-Carrion et al., 2006, Rutherford, Ojeda et al., 2005, Ueta, Fujiwara et al., 2012).

Subsequently, several studies have reported that, besides the capacity of Grx3/4 to bind an Fe–S cluster into homodimers, they can also form [2Fe–2S] cluster-bridging heterodimeric complexes with Fra2 (Li et al., 2009). Interestingly, Fra2 converted the [2Fe–2S] Grx3 homodimer to [2Fe–2S] Grx3–Fra2 heterodimer, this conversion being thermodynamically and kinetically favored (Li, Mapolelo et al., 2011).

Aft2 can bind a [2Fe–2S] cluster into a dimer and that it only interacts with and accepts an Fe–S cluster from a [2Fe–2S] loaded Fra2–Grx3 complex but not from a [2Fe–2S] cluster bound form of a Grx3–Grx3 homodimer (Fig I-7) (Poor, Wegner et al., 2014). Overall, it was concluded that the DNA affinity of the [2Fe–2S] loaded Aft2 is decreased, which promotes its nuclear export, preventing as explained above its ability to activate the iron regulon (Fig I-7). The fact that Aft1/2 is only partially repressed in the fra2 mutant under iron-replete conditions suggests that a Grx3/4 holo-homodimer may be able to transfer Fe–S cluster to Aft1/2 *in vivo* although less efficiently (Kumanovics et al., 2008).

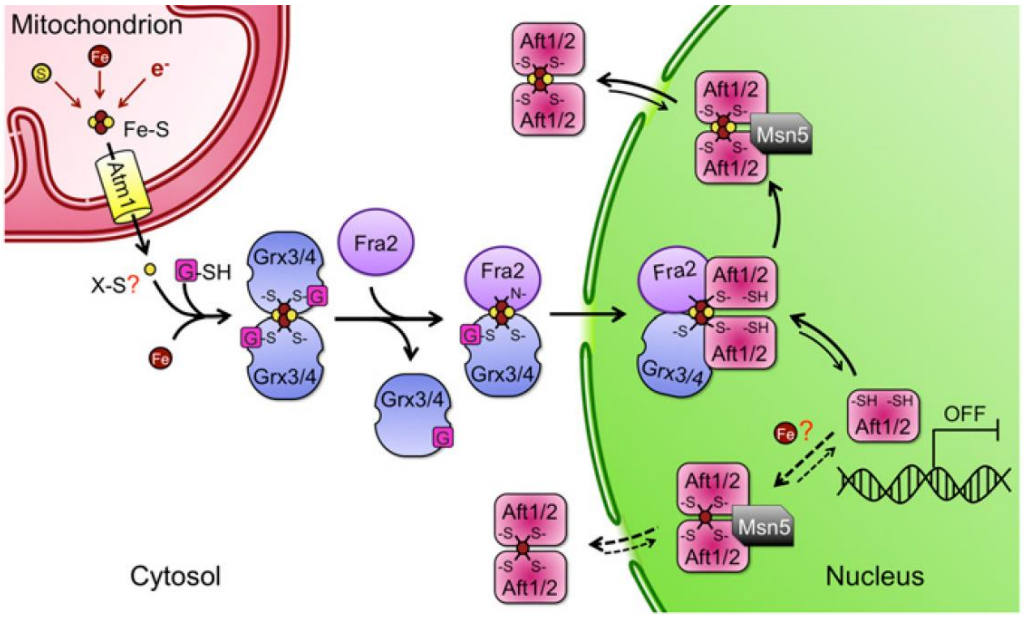
Mitochondrion
Fe
S
e-
Fe-S
Atm1
X-S?
G-SH
Fe
Grx3/4
Grx3/4
Fra2
Fra2
N-
Grx3/4
Grx3/4
Aft1/2
Aft1/2
Aft1/2
Msn5
Aft1/2
Fra2
Aft1/2
Grx3/4
Aft1/2
-SH -SH
Aft1/2
OFF
Fe?
Aft1/2
Msn5
Aft1/2
Aft1/2
Aft1/2
Cytosol
Nucleus

Fig I-7. Proposed model for iron regulation via Aft1 and Aft2 under iron replete conditions (Poor, C. et al., 2014)

During conditions of iron sufficiency, Fe–S clusters are synthesized in mitochondria via integration of iron, sulfur, and redox control pathways. An unknown substrate produced by the mitochondrial Fe-S cluster biogenesis machinery is exported to the cytosol by the transporter Atm1. GSH is also required for export of this signal. Grx3 and Grx4, which form GSH ligated, Fe-S–bridged homodimers, are proposed to form heterodimers with Fra2 to relay this signal to Aft1 and Aft2. Interaction of Grx3/4 with Aft1 promotes dissociation of the transcriptional activator from its target DNA and export to the cytosol, leading to deactivation of Aft1/2-regulated genes. The exportin Msn5 facilitates iron-dependent export of both Aft1 and Aft2.

I.4.3. Role of Grx4 and Fra2 in iron homeostasis in *S. pombe*

Inactivation of the grx4+ gene (grx4Δ) generates a constitutively active Fep1 that binds to its target gene promoters in vivo. In the absence of Grx4, Fep1 behaves like an insensitive protein, constitutively repressing target gene expression (Jbel et al., 2011). Although the molecular basis by which Grx4 communicates iron deficiency to Fep1 remains obscure, two-hybrid and co-immunoprecipitation experiments have revealed that the TRX domain of Grx4 associates strongly and constitutively with the C-terminal region of Fep1. Additional analyses have shown that, under low but not high-iron conditions, the GRX domain of Grx4 associates with the N-terminal region of Fep1, which contains its DNA-binding domain. A possible mechanism for iron starvation-dependent inactivation of Fep1 by Grx4 would be that Fep1-GRX domain interaction triggers conformational changes that impair Fep1 DNA binding, thus blocking its association with chromatin and its repressive effect on target gene expression (Fig I-1)

One additional molecule has lately been reported to play a role in Fep1 inactivation in response to iron deficiency (Encinar del Dedo, Gabrielli et al., 2015, Jacques, Mercier et al., 2014). In *S. pombe*, the fra2+ gene encodes a BolA2-like protein, which has been shown to form a [Fe-S]-bridged complex with the multidomain CGFS monothiol glutaredoxins Grx4 (Encinar del Dedo et al., 2015). Disruption of fra2+ (fra2Δ) causes a constitutive repression of iron transport genes and leads to constitutive promoter occupancy by Fep1 where it mediates its repressive effect (Encinar del Dedo et al., 2015, Jacques et al., 2014). In *S. pombe*, Fra2 and Grx4 are distributed throughout the cells with a significant proportion of the two proteins located in the nuclei (Jacques et al., 2014). Co-immunoprecipitation experiments have revealed that Fra2, Fep1 and Grx4 are associated in a heteroprotein complex. Bimolecular fluorescence complementation (BiFC) experiments have brought further evidence that an interaction between Fep1 and Fra2 occurs in the nucleus.

I.5. Biology of *Schizosaccharomyces pombe*

I.5.1. The early research and phylogeny of *S. pombe*

In 1893, Lindner discovered *Schizosaccharomyces pombe* in East African millet beer, locally called 'pombe'. The strain currently used for genetic research was isolated by Urs Leupold (University of Berne, Switzerland) in 1950 from a grape-derived yeast culture of the 'Centraalbureau voor Schimmelcultures' (Central depository for fungi cultures) in the Netherlands.

The fission yeast *S. pombe* is proving increasingly attractive as an experimental system for investigating problems of eukaryotic cells and molecular biology. Many of the powerful molecular genetic procedures developed for *Saccharomyces cerevisiae* can now be applied to *S. pombe* (Moreno, Klar et al., 1991). The single genus *Schizosaccharomyces* embraces a small group of possibly quite divergent ascomycete yeasts that share the common feature of division by medial fission. With the exception of *S. pombe*, the fission yeasts are studied relatively little. However, the relationships between the various members of the group have been clarified (Sipiczki, 1989). *S. pombe* and *S. malidevorans* produce four spore asci. Since these strains are cross-fertile, they are, strictly speaking, varieties of a single species, i.e., *S. pombe* var. *pombe* and *S. pombe* var. *malidevorans*. *S. octosporus* and *S. japonicus* produce eight spore asci, and the latter species is also subdivided into two varieties, *S. japonicus* var. *japonicus* and *S. japonicus* var. *versatilis*, on the basis of their growth form.

S. pombe is classified as a fungus, namely an ascomycete fungus characterized by the formation of an ascus. Over the past century, ascomycete fungi have been reclassified frequently, based on various phenotypic characteristics, such as the shape of the ascospore, type of cell division (budding vs. fission), presence of hyphae, ability to ferment certain sugars or grow on various carbon and nitrogen sources. Recently, DNA and RNA sequence analyses have been used to determine

sequence divergence among ascomycete fungi and, thus, to quantitate genetic differences between species. These molecular techniques demonstrate that fission yeast *S. pombe* is phylogenetically as distant from budding yeasts as it is from humans. The *Schizosaccharomyces* lineage separated about 1 billion years ago to form an ancestral branch of the ascomycetes, denoted archaeascomycetes. However, the view that *S. pombe* maps to a different part of the tree than expected is supported by phylogenetic analyses using mitochondrial sequence data. The universal translation code is used for all ubiquitous mitochondrial genes of *S. pombe*, which clearly distinguishes it from other ascomycetes that have one or more codon reassignments. The universal translation code is also used in mitochondria of several lower fungi, such as the zygomycetes (e.g., *Rhizopus stolonifer*) and certain lineages of the chytridiomycetes (e.g., *Allo-myces*, belonging to the Blastocladiales; as well as *Monoblepharella* and *Harpo-chytrium*, belonging to the Monoblepharidales). The universal translation code in *S. pombe* can be explained as a primitive character inherited from its lower fungal ancestors. In view of this special position of *S. pombe* within the ascomycetes, the common name "fission yeast" is misleading, because it has not more in common with budding yeasts (e.g., *Saccharomyces*, or *Pichia*) as have non-yeast ascomycetes (e.g., *Neurospora* or *Penicillium*). Despite its use of a mitochondrial universal translation code, however, the tiny *S. pombe* mitochondrial genome rather reflects a very derived fungus.

I.5.2. Life cycle of *S. pombe*

During its normal life cycle, fission yeast cells are haploid, meaning that they have only one copy of each chromosome. Haploid yeast cells are used for research because both recessive and dominant mutations will result in mutant phenotype. Haploid cells multiply asexually through mitosis. Newly born daughter cells grow at the tips of their cylindrical rod shape. When they have grown to a mature length,

cells stop growing and produce septa in the middle of the cells. The septum divides the mother cell into two equal-size daughter cells. In rich medium, the daughter cells will separate to start over the haploid cell cycle; each haploid cell cycle takes about 3 hours (In contrast, the mammalian cell cycle takes about 24 h). In the wild, yeast cells often live under nutrient-deprived conditions. Because *S. pombe* is a dimorphic yeast, it can switch from a yeast-form morphology to a pseudo-hyphal morphology, in which the daughter cells remain attached. Pseudo-hyphal growth allows the cells to spread out more efficiently and forage for fresh nutrients.

S. pombe has two opposite mating types, namely '+' and '-' mating types. When rich conditions are followed by starvation conditions, haploid yeast-form cells of the opposite mating type will conjugate pair-wise and fuse at their tips. Subsequently, the nuclei will fuse to form diploid cells, called zygotes. Usually, zygotes undergo meiosis immediately, followed by sporulation and formation of four-spore zygotic asci. The ascus wall will auto-lyse, liberating the haploid ascospores, which are able to survive long periods of stress. When environmental conditions become favorable for growth, the spores will germinate and the haploid cell cycle will begin again. If zygotes encounter rich conditions, they infrequently can undergo mitosis instead of meiosis and enter the diploid cell cycle.

Diploid cells divide by medial fission, like haploid cells, but are longer and wider than haploid cells. Haploid cells measure 7-8 (newly born) to 12-15 μm (at division) in length and 3-4 μm in width, while diploid cells measure 11-14 (newly born) to 20-25 μm (at division) in length and 4-5 μm in width. Diploid cells will continue mitotic growth until nutrients run out. Then, they undergo meiosis and form azygotic asci, containing four haploid ascospores. After environmental condition become favorable for growth, the spores will germinate and the normal haploid cell cycle will begin.

I.5.3. Genomic information of *S. pombe*

The fully annotated genome sequence of *S. pombe* has been completed (WoodGwilliam et al., 2002). It becomes the sixth eukaryotic genome to be sequenced, following *Saccharomyces cerevisiae, Caenorhabditis elegans, Drosophila melanogaster, Arabidopsis thaliana,* and *Homo sapiens*. The 13.8 Mb genome of *S. pombe* is distributed between chromosomes I (5.7 Mb), II (4.6 Mb) and III (3.5 Mb), together with a 20 kb mitochondrial genome. It contains the smallest number of protein-coding genes yet recorded for a eukaryote: 4,824 genes (including 11 mitochondrial genes), substantially less than the 5,570 ~ 5,651 genes predicted for *S. cerevisiae*, the 6,752 genes predicted for *Mesorhizobium loti*, the largest published prokaryote genome sequence to date, and the 7,825 genes estimated in the 8.67 Mb genome of the prokaryote *Streptomyces coelicolor* (Wood et al., 2002).

Fig. I-8. Life cycle of fission yeast *S. pombe*

('www information on *Schizosaccharomyces pombe* by Frans Hochstenbach at the University of Amsterdam' (*http://www.bio.uva.nl/pombe/cycle/lifetext.html*))

A. Haploid cells multiply asexually through mitosis.

B. Pseudo-hyphal morphology cells.

C. Conjugation of two different mating type cells.

D. Formation of zygotes, the diploid cells.

E. Formation of four-spore zygotic asci.

F. Spore germination.

G. Diploid cells divided by medial fission.

H. Diploid cells are longer and wider than haploid cells.

I. Formation of azygotic asci.

J. Life cycle of fission yeast. (top left) Haploid mitotic cell cycle; (center and lower left) haploid cells mating to form a diploid zygote, followed by meiosis and sporulation leading to zygotic ascus formation; (lower right) re-entry of diploid zygotes into mitotic cycle (copied from MacNeill and Nurse, 1997).

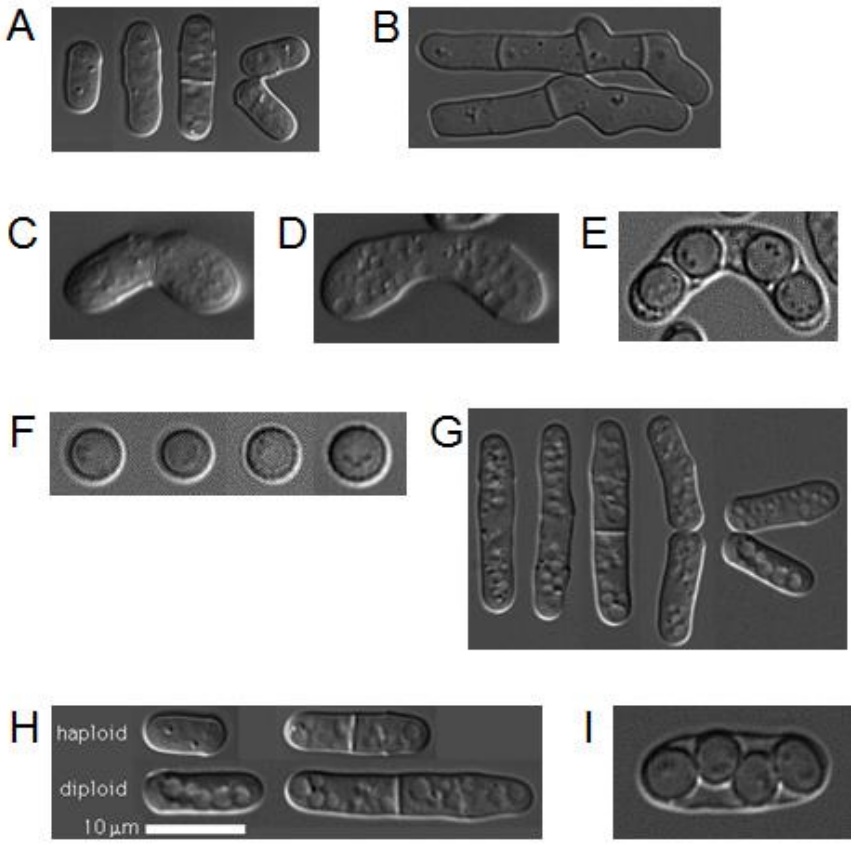
A
B
C
D
E
F
G
H
haploid
diploid
10 µm
I
J
Stationary phase
Nutrient deprivation
Haploid mitotic cell cycle
Conjugation between haploid cells of opposite mating type
Re-supply nutrients
Zygote formation
Re-supply nutrients
Nutrient deprivation
Meiosis and sporulation
Diploid mitotic cell cycle
Meiosis and sporulation
Dormant ascospores
Zygotic ascus
Azygotic ascus

I.6. Aims of this study

How iron-responsive gene expression is mechanistically linked to the fitness of mitochondrial ISC assembly is based on the assumption that fungal iron-responsive transcription factors are Fe/S proteins. Their Fe/S co-factor is assembled in a Grx4-dependent manner, which is supported by the fact that monothiol glutaredoxins play a central role in cytosolic iron metabolism and easily transfer their own bound Fe/S cluster to target apo-proteins *in vitro* (Muhlenhoff et al., 2010, Rouhier et al., 2010).

So far, it has not been demonstrated that Aft1, Fep1 or Php4 bind Fe/S clusters when purified from their native host. Evidence for Fe/S cluster binding to these regulators is based on *in vitro* analysis of recombinant proteins only. The Fep1 homolog SRE from *Neurospora crassa* binds iron when purified from *Escherichia coli* (Harrison & Marzluf, 2002). The bound co-factor was poorly characterized, but the UV–vis spectrum was indicative of an Fe/S cluster. Iron binding involved a cysteine pair that is essential for iron sensing and highly conserved in the Fep1 ortholog SreA of ascomycetes (Schrettl et al., 2008). The Fep1 ortholog Sre1 from *Histoplasma capsulatum* also bound sub-stoichiometric amounts of iron, but whether the recombinant protein bound iron in form of an Fe/S cluster was not thoroughly analyzed (Chao et al., 2008). However, binding to target promoters *in vitro* was induced by ferric iron, indicating that iron alone is sufficient for iron-responsive regulation by Sre1.

A recent study reported that Fep1 binds iron, but not as an Fe-S cluster form (Encinar del Dedo et al., 2015). It also demonstrated that Grx4-Fra2 complex can bind [Fe-S] and facilitates iron transfer from Fep1 to Grx4-apo-Fra2. This supports a model that iron starvation causes dismantling of [Fe-S] from the Grx4-Fra2 complex and facilitates iron transfer from Fep1 to Grx4-Fra2, inactivating Fep1 function. However, numerous questions remain unresolved, regarding the type of

iron cofactor in Fep1, and the mechanism of iron transfer between Fep1 and Grx4-Fra2. In this study, I pursued biochemical and spectroscopic analyses of Fep1, in full length and truncated forms, as isolated or reconstituted proteins, with the wild type or substituted cysteine mutations.

CHAPTER II.

MATERIALS AND METHODS

II.1. Strains and plasmids construction

For N-terminal hexa-histidine tagging, the full length and N-terminal half (1-238 aa) of the *fep1*$^{+}$ gene in *S. pombe* were amplified by PCR from the chromosomal DNA as a template. The PCR products were cloned into pET15b vector (Novagen) via *Nde*1 and *Bam*H1 sites, resulting in pET15b-Fep1 or pET15b-Fep1-N238 or pET15b-Fep1-N114. The cysteine mutant Fep1-N238 2CS (C85S/C88S), Fep1-N238 4CS (C70S/C76S/C85S/C88S) was generated by PCR mutagenesis and cloned into pET15b. All constructs were confirmed by nucleotide sequencing.

II.2. Protein expression and purification

The His-tagged recombinant proteins of full-length Fep1, Fep1-N238, and Fep1-N238 4CS were expressed in *E. coli* BL21 (DE3) grown in LB at 37°C to OD_{600} of 0.5~0.6, followed by induction with 1 mM IPTG for 5 h. Harvested cells were lysed at 4°C in the binding buffer (20 mM Tris-HCl, pH 8.0, 500 mM NaCl, 5 mM imidazole) by using a high-pressure homogenizer EmulsiFlex-C3 (Avestin). Following centrifugation at 15000 *g* for 15 min at 4°C, the cell-free extracts were loaded onto Ni-IDA (iminodiacetic acid) column (ELPIS) pre-equilibrated with the binding buffer, and eluted with 500 mM imidazole. The partially purified proteins were then applied to HiLoad Superdex 75 column (GE Healthcare), followed by elution with 20 mM Tris-HCl buffer containing 500 mM NaCl and 1 mM DTT. For anaerobic purification, Ni-affinity chromatographies were done in the anaerobic glove box (O_2 < 2 ppm; Coy Laboratory Products, Inc.).

II.3. Transformation of *Escherichia coli* and Yeast

For the purpose of general cloning, *E. coli* DH5α competent cells were used for transformation by heat shock method (42°C for 1 min 30 sec.). High efficiency

electroporation method of *E. coli* (XL1-Blue) was used to amplify *S. pombe* genomic library plasmid of interesting target gene from the purified yeast total genomic DNA.

The *S. pombe* transformation was routinely done using lithium acetate (LiAc) / Polyethylene glycol (PEG) method according to Moreno *et al*. (1991).

II.4. Western blot analysis

Western blot analyses were performed *E. coli* cells were cultured and harvested at certain growth phase. Total cell extracts or fractionated extracts were resolved in SDS-PAGE (10 ~ 18%). Gel was transferred onto PROTRAN (nitrocellulose transfer membrane; Schleicher & Schuell) using TransBlot system (BioRad) at 160 ~ 180 mA for 50 min.

Filters with bound protein were washed 3 times and blocked in 10 ml of Tris-buffered saline containing 0.1% Triton-X 100 (TBS-T) with 0.5% BSA. Filters were incubated for 1 hr with proper antibodies in TBS-T containing 0.5% BSA. Excess antibodies were removed by repeated washing in TBS-T. After 1 hr incubation in TBS-T containing the secondary antibody conjugated with horseradish peroxidase, the signal was visualized with LAS3000 (Fuji) and quantified with Multi Gauge (Fuji) program.

II.5. Preparation of apoprotein

Apo-Fep1-N238 was prepared by incubating the iron-bound as-isolated Fep1-N238 (100 μM) in 20 mM Tris-HCl buffer (pH 8.0) containing 500 mM NaCl, 10 mM EDTA, and 5 mM sodium dithionite (SDT) for 1 h on ice. The colorless protein solution was then buffer-exchanged into 20 mM Tris-HCl, pH 8.0, 500 mM NaCl through two consecutive PD10-desalting columns (GE Healthcare).

II.6. Fe-S cluster reconstitution *in vitro*

Reconstitution of Fe-S cluster into full-length Fep1 or Fep1-N238 was performed anaerobically (O_2 < 2 ppm) in a glove box (Coy Laboratory Products, Inc.). Following incubation of 50~100 µM apo-Fep1-N238 with 2 mM DTT for 30 min, 5-fold molar excess of ferric chloride ($FeCl_3$) and sodium sulfide (Na_2S) were added and incubated for 2 h at room temperature. The reconstitution mixture was subjected to two consecutive chromatographies in the glove box through PD10-desalting column equilibrated with 20 mM Tris-HCl and 500 mM NaCl, to remove excess iron and sulfide.

II.7. Assays for quantification of iron, sulfide and protein

II.7.1. Determination of iron concentration

The amount of iron in the purified protein sample was determined by using colorimetric ferrozine assay (Riemer, Hoepken et al., 2004). Aliquots (100 µL) of proteins were placed in Eppendorf tubes and mixed with 100 µL of 10 mM HCl (the solvent of the iron standard FeCl3), and 100 µL of the iron-releasing reagent (a freshly mixed solution of equal volumns of 1.4 M HCl and 4.5% (w/v) KMn04 in H2o). These mixtures were incubated for 2 h at 60°C. The HCl/ KMnO4-mediated digestion of iron-containing proteins is essential for iron quantitation of proteins. After the mixtures had cooled to room temperature, 30 µL of the iron-detection reagent (6.5 mM ferrozine, 6.5 mM neocuproine, 2.5 M ammonium acetate, and 1 M ascorbic acid dissolved in water) was added to each tube. After 30 min, 280 µL of the solution in each tube was transferred into a well of a 96-well plate and the absorbance was measured at 550 nm on a microplate reader.

II.7.2. Determination of sulfide concentration

Acid labile sulfide concentration was determined by using methylene blue-based color assay as described previously (Beinert, 1983). The tubes were kept tightly capped except when adding reagents. Rather than using stir bars, the tubes were closed and vortexed when mixing was called for. The procedure used was as follows. The sample volumes were brought to 100mL with pH 8 water. One at a time, each tube was opened, 300 mL 1% ZnOAc and 15 mL 12% NaOH were added simultaneously, the tube was closed tightly and vortexed. When all tubes had been treated in this way, they were allowed to sit for 15 min before addition of 75 mL DMPD (0.1% in 5 N HCl) and 2 mL FeCl3 (23 mM in 1.2 N HCl). Using Na2S z 9H2O as a standard as described by Beinert, this method proved very reproducible in our hands. In this assay, N,N-dimethyl-p-phenylenediamine (DMPD) is converted to methylene blue (MB) in the presence of sulfide and $FeCl_3$. Precautions were made to avoid residual amount of reducing agent such as DTT in the buffer that could hinder oxidation of DMPD by $FeCl_3$.

II.7.3. Determination of protein concentration

Protein concentrations were determined by infrared-based peptide quantification system, using Direct Detect infrared spectrometer (Merck Millipore). Bovine serum albumin (BSA) was used as a standard.

II.8. EPR spectroscopy

Fresh Fep1-N238 samples purified anaerobically were equilibrated in 20 mM Tris-HCl buffer containing 500 mM NaCl, 1 mM DTT, and 10% (v/v) glycerol in the glove box. Fep1 proteins were either non-treated or treated with sodium dithionite (10 mM final) or ferricyanide (5 mM final), and transferred to EPR tubes. Following

10 min incubation at room temperature, the EPR tubes were frozen in liquid nitrogen. EPR measurements were carried out at Korea Basic Science Institute (KBSI), Western Seoul Center, for low temperature (5 K) analysis. CW X-band (9.6 GHz) EPR spectra were collected on a Bruker EMX plus 6/1 spectrometer equipped with a liquid helium cryostat (ESR900, Oxford Instrument) and ITC 503 temperature controller. All spectra were collected with the following experimental parameters: microwave frequency, 9.6 GHz; microwave power, 1 mW; modulation amplitude, 10 G; time constant, 20.48 ms; 5 scans. For measurements at liquid nitrogen temperature (123 K), samples were subjected to ESR spectrometer (JES-TE200, JEOL) at National Instrumentation Center for Environment Management (NICEM), Seoul National University.

CHAPTER III.
RESULTS & DISCUSSION

III. 1. Purification and UV-visible absorption spectroscopy of full-length Fep1

III. 1. 1. Purification of full-length Fep1

Aiming at identifying biochemical characterizations of Fep1 protein, His-tagged full length Fep1 (564 aa) was overproduced in *E. coli* and anaerobically purified through Ni-IDA affinity column. Multiple protein bands were observed on SDS-PAGE at 70 kDa and 30-35 kDa size ranges (Fig. II-2A). LC-MS/MS analysis identified that 30-35 kDa bands are degraded products of Fep1. A Western blot assay using 6His-probe Antibody confirmed that bands of SDS-PAGE were 6His-tagged full length Fep1 and 6His-tagged Fep1 degraded products (Fig. II-2B). To remove the degraded Fep1 fragments and other possible contaminating proteins, gel filtration chromatography was performed on Superdex 75 column, equilibrated with 20 mM Tris-HCl, pH 8.0, 500 mM NaCl, 1 mM DTT. Finally, we could successfully isolate full-length Fep1 only. The single-peaked fractions centered around 128 kDa position were collected (Fig. II-2C, red bracket) and subjected to SDS-PAGE to confirm purification of the full-length Fep1. A prominent single band was observed, coinciding with the calculated mass of 62.9 kDa with a hexa-histidine tag (Fig. II-2D). The gel filtration behavior fits with the previous report that Fep1 can dimerize through C-terminal region of Fep1 (Pelletier et al., 2005). As demonstrated in Fig. II-2D, the purified full length protein did not undergo further degradation, when it was concentrated through centricon (Millipore) in the air, and kept at 4°C in the refrigerator or in the anaerobic glove box for 19 h (lanes 2-4).

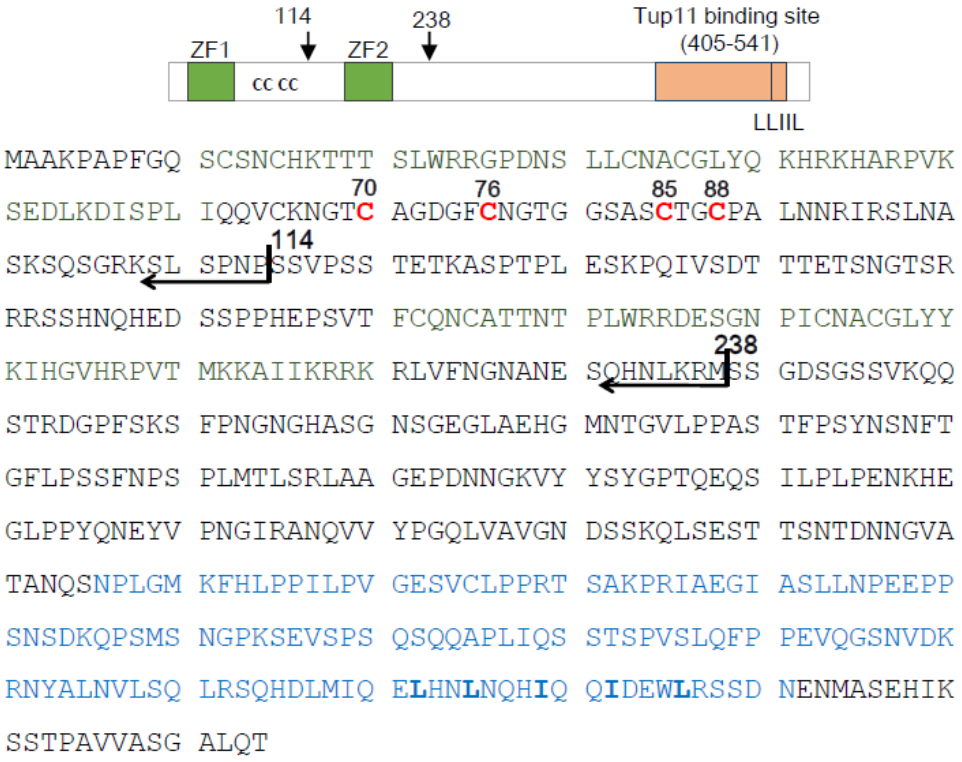

Fig II-1. Domain structure of Fep1 in *S. pombe*

Localization of Zinc finger (ZN) motifs and conserved cysteine residues within the sequence.

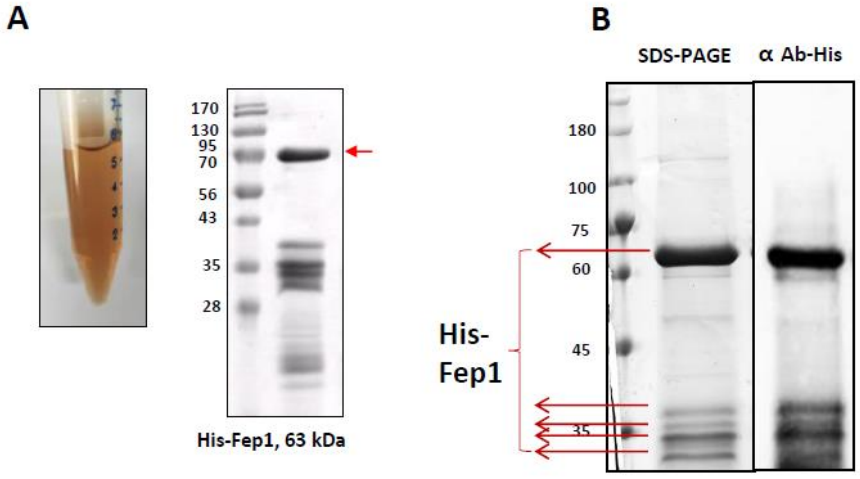

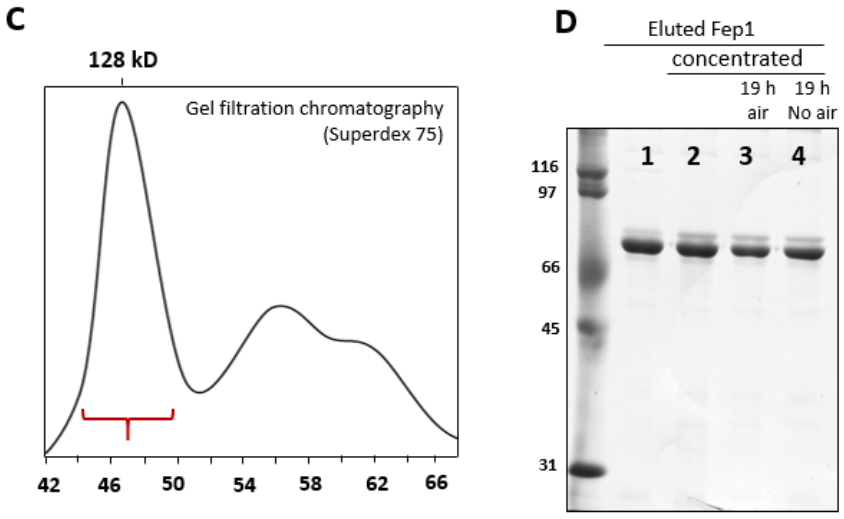

E

Ni -affinity	color	Gel filtration chromatography	color
Aerobic	Red	Aerobic	-
Aerobic	Red	Aerobic (DTT)	Red
Anaerobic	Red	Anaerobic	-
Anaerobic	Red	Anaerobic (DTT)	Red

Fig II-2. Purification of full-length His-tagged Fep1.

A. Anaerobically purified Fep1 by Ni-agarose column.

B. LC-MS/MS analysis showed that multi-bands of SDS-PAGE were degraded products of expressed Fep1. A Western blot assay using 6His-probe Antibody (Santa cruz, sc 804) confirmed that bands of SDS-PAGE were 6His-tagged full length Fep1 and 6His-tagged Fep1 degraded products.

C. D. A gel filtration chromatogram of Fep1 protein, following Ni-affinity column. From Superdex 75 column, the full length Fep1 is eluted as a single peak, with the median elution volume (Ve) of 47 ml, which corresponds to 128 kDa determined by standard size marker proteins. Degraded Fep1 fragments were eluted later. The purity and stability of full-length Fep1 was monitored by SDS-PAGE. The freshly eluted Fep1 (lane 1) was concentrated by Centricon (Millipore) (lane 2), and stored either in the air (lane 3) or in the anaerobic glove box (O_2 < 2 ppm; lane 4) for 19 hours.

E. Effect of DTT on Fe binding stability of Fep1 during purification

III. 1.2. UV-visible absorption spectroscopy of full-length Fep1

During Ni-affinity purification, Fep1 protein showed reddish brown color. During gel filtration, the reddish color disappeared in the absence of DTT. Therefore 1 mM DTT was added in the buffer throughout the chromatography (Fig. II-2E). The UV-visible absorption spectra were recorded immediately after purification for both anaerobically and aerobically prepared samples. The aerobically purified Fep1 also showed similar reddish brown color and nearly identical absorption behavior. The absorption spectra demonstrated peaks at 320 and 420 nm, and a shoulder around 520 nm for both samples, characteristic of Fe-S-containing proteins (Fig. II-3A). The absorption spectra looked quite similar to that of purified recombinant SRE (Harrison & Marzluf, 2002), a Fep1 homologue in *Neurospora crassa*. Molar extinction coefficients (ε) at 420 nm based on the concentration of the purified Fep1 was 3.0 $mM^{-1}cm^{-1}$. (Fig. II-3A).

To further examine the oxygen lability of its Fe-binding, I observed UV-visible spectra of anaerobically purified Fep1 depending on the time in the presence of oxygen. Fep1 showed stable spectra at least for several hours (Fig. II-3B). These results suggest that the iron-binding in the purified Fep1 is relatively stable in DTT-containing buffer during several hours of aerobic purification procedures. I also found that the absorption peaks at 320, 420, and 520 nm all disappeared when treated with 5 mM sodium dithionite, a strong reductant (Fig. II-4). These spectrophotometric observations indicate that the purified, as isolated Fep1 contains redox-active iron, possibly in the Fe-S cluster form. Upon reconstitution, UV-visible absorption was significantly enhanced (Fig. II-5, *red line*), but shape of absorption spectra

was similar to as-isolated Fep1 (Fig. II-5, *gray line*). After reconstitution of full-length Fep1, molar extinction coefficients (ε) at 420 nm was 5.2 $mM^{-1}cm^{-1}$ (Fig. II-5).

III.2. Fep1-N238 binds an Fe-S cluster via four conserved cysteine residues

III.2.1. Purification and UV-visible absorption spectroscopy of Fep1-N238

Since Fep1 undergoes extensive degradation during Ni-affinity purification procedure, resulting in low yield of full length proteins, I constructed and purified truncated forms of Fep1 that contains N-terminal 238 aa and 114 aa (Fig II-6). Fep1-N238 contains a conserved cysteine-rich region between two consensus zinc finger motif that is critical region to DNA-binding and the inhibition mechanism (Jbel et al., 2011). Fep1-N114 doesn't have second zinc finger motif (ZF2). 6His-tagged wild type Fep1-N238 and Fep1-N114 overproduced in *E. coli* cells showed reddish brown color, suggesting the possibility that iron cofactor might be involved in the overproduced proteins (Fig II-7). As expected, the purified Fep1-N238 and Fep1-N114 proteins also were reddish color. Purified Fep1-N238 (28.1 kDa with His-tag) and Fep1-N114 (13.5 kDa) by nickel affinity agarose and gel filtration column were confirmed on SDS-PAGE gel (Fig II-8). The UV-visible absorption spectrum of Fep1-N238 looked almost identical to that of the full length Fep1 (Fig II-9A) and it was unaffected by absence of second zinc finger (ZF2). It suggest that the iron-binding property of Fep1 resides in the N-terminal region, and is not significantly affected by the C-terminal

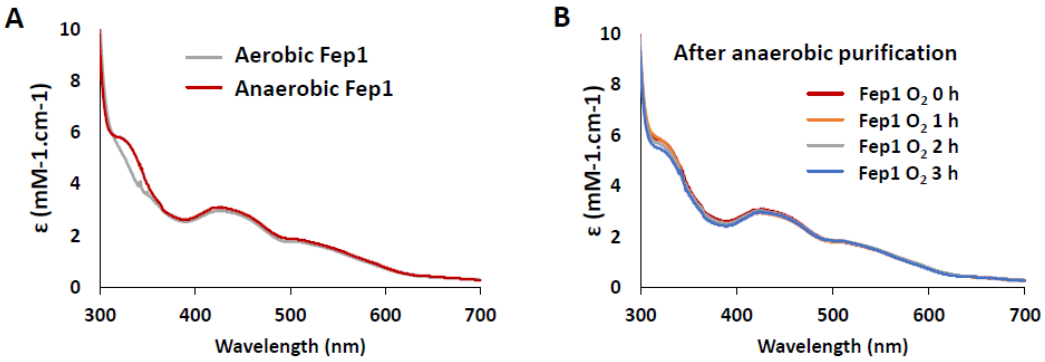

Fig II-3. Effect of oxygen on stability of Fe binding on full-length Fep1

A. UV-visible absorption spectra of full-length Fep1, purified anaerobically (red line) or aerobically (gray line). Absorbance was presented as molar extinction coefficient (ε) to normalize protein content in each sample.

B. Time-course of absorption spectra of anaerobically purified Fep1 after exposure to air for the times indicated.

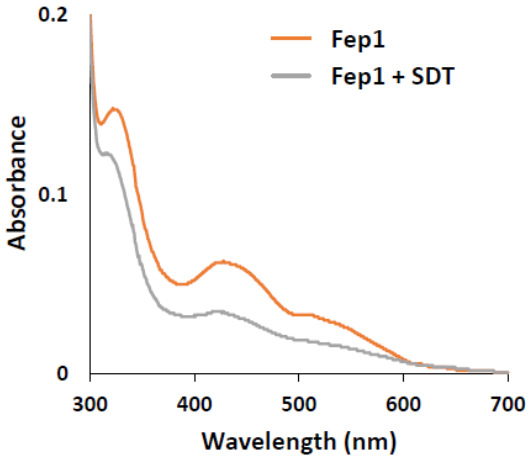

Fig II-4. UV-visible absorption spectra of reduced full-length Fep1

Anaerobically purified full-length Fep1 (orange line) was reduced by sodium dithionite (SDT; gray line).

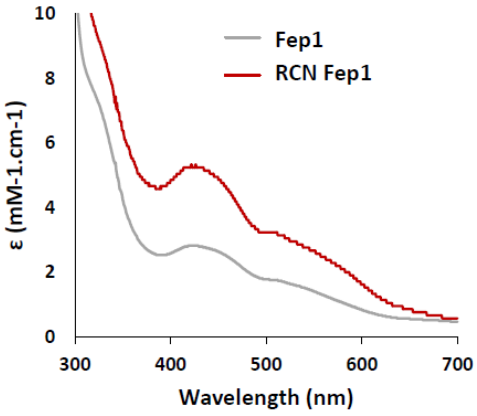

Fig II-5. UV-visible absorption spectra of reconstituted full-length Fep1

UV-visible absorption spectra of as-isolated Fep1 (*gray line*) and chemical reconstituted Fep1 (*red line*). Absorbance was presented as molar extinction coefficient (ε) to normalize protein content in each sample.

half of Fep1. The visible spectra of wild type Fep1-N238 did not change for several hours even without dithiothreitol (DTT), suggesting that the Fep1-N238 protein has relatively more stable Fe-S cluster in oxidation condition than full-length Fep1 (Fig II-9B). We therefore pursued further experiments with the Fep1-N238.

After aerobically-purified wild-type Fep1-N238 was equilibrated under anaerobic conditions (O_2 < 2 ppm), sodium dithionite (20 mM final concentration) was added. Anaerobic reduction of Fep1-N238 protein by dithionite partially bleached its visible absorbance (Fig II-10A, *gray line*). This observation indicates that Fep1-N238 has redox-active metal cofactor most likely Fe-S cluster. After reconstitution of Fep1-N238, molar extinction coefficients (ε) at 420 nm was increased from 2.7 $mM^{-1}cm^{-1}$ to 6.9 $mM^{-1}cm^{-1}$ (Fig II-10B).

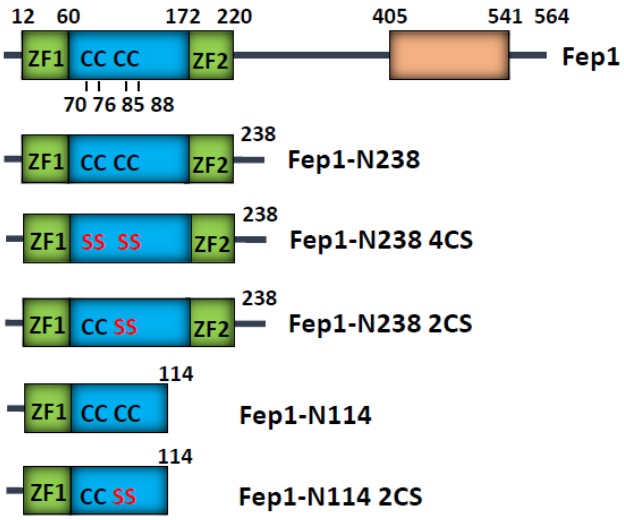

Fig II-6. Schematic presentations of the wild-type and the cysteine mutant Fep1 used in this study.

In the N-terminal DNA-binding domain, two GATA-type zinc finger motifs (ZF1 and ZF2; green) flank the central region that contain four cysteines conserved among Fep1-like proteins. In the C-terminal region resides a Tup11-interacting domain (405-541; orange). The truncated N238 proteins with wild type or four cysteine substitutions (4CS) were depicted.

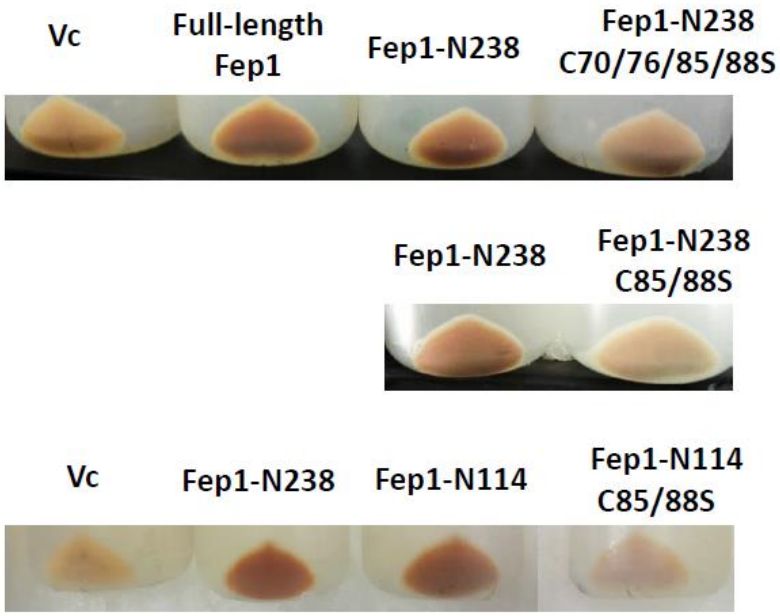

Fig II-7. Reddish brown color of Fep1-overexproduced cell

Escherichia.coli BL21 (DE3) were transformed with pET15b vector (Vc), recombinant Fep1 WT (full-length, truncated Fep1) and their conserved cysteine mutants C85S/C88S (2CS), C70S/C76S/C85S/C88S (4CS). Cells were incubated in 1 mM IPTG at 30℃ for 5 h. Fep1 WT proteins overexpressed cell showed reddish brown color, while cysteine mutants Fep1-N238 2CS, Fep1-N238 4CS, Fep1-N114 2CS were shown significantly decreased reddish color.

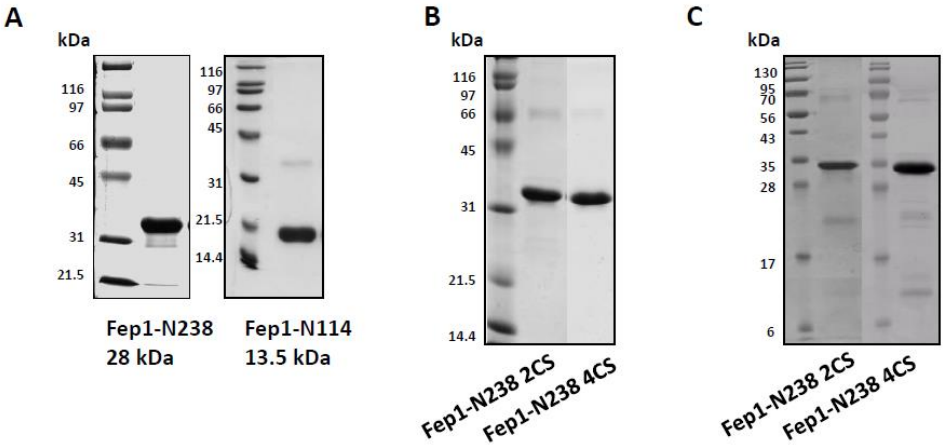

Fig II-8. SDS-PAGE analysis of truncated variant Fep1 proteins

The purified variant Fep1 proteins were determined by SDS-PAGE analysis.

A. His-Fep1-N238 and His-Fep1-N114 purified by Gel filtration chromatography.

B. His-Fep1-N238 2CS and His-Fep1-N238 4CS purified by Gel filtration chromatography.

C. His-Fep1-N238 2CS and His-Fep1-N238 4CS purified by Ni-affinity column

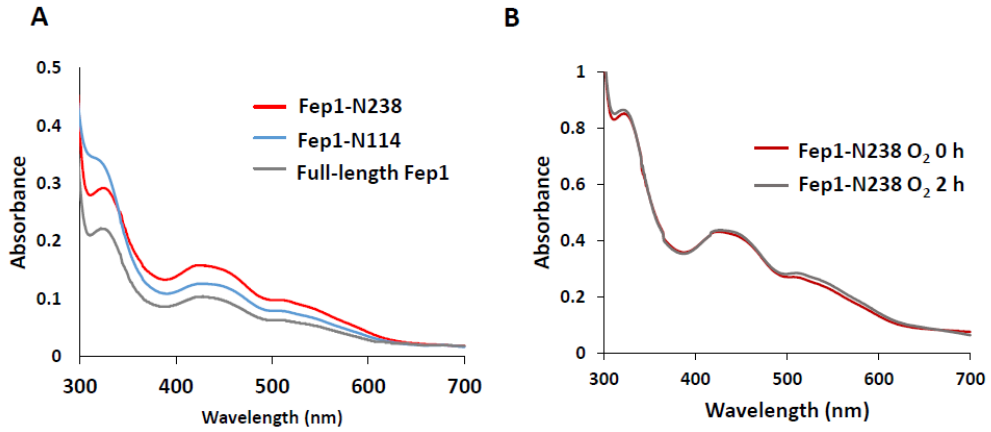

Fig II-9. UV-visible absorption spectra of Fep1-N238 & Oxygen stability

A. UV-visible absorption spectrum of anaerobically purified Fep1-N238 and Fep1-N114 in comparison with full-length Fep1.

B. Effect of oxygen on stability of Fe binding on aerobically purified Fep1. Time-course of absorption spectra of aerobically purified Fep1-N238 after exposure to air.

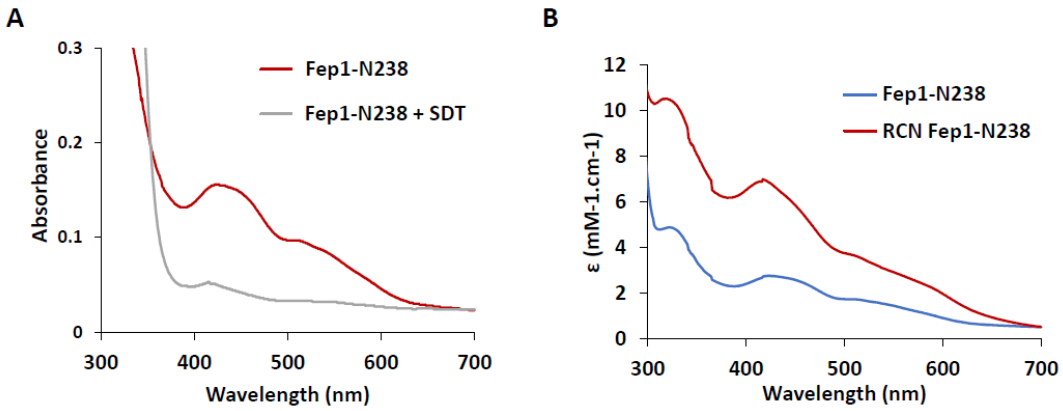

Fig II-10. UV-visible absorption spectra of reduced & reconstituted Fep1-N238

A. Absorption spectra of the sample as-isolated in the oxidized form (*red line*) and the reduced form after the addition of 20 mM sodium dithionite (*gray line*) were anaerobically (O_2 < 2 ppm) recorded at room temperature.

B. UV-visible spectra of as-isolated Fep1-N238 and reconstituted (RCN) Fep1-N238. Absorbance was presented as molar extinction coefficient (ε) to normalize protein content in each sample.

III. 2.2. Purification and UV-visible absorption spectroscopy of Fep1 cysteine mutants

To verify that four conserved cysteine residues are involved in coordination of Fe-S cluster, four cysteine residues in Fep1-N238 was individually mutated to serine (C70S/C76S/C85S/C88S) designated Fep1-N238 4CS. We also created a mutant Fep1 where the conserved two cysteines (C85, 88) that is necessary for iron-mediated repression of *fio1*$^{+}$ expression (Pelletier et al., 2005) were changed to serines. In contrast to wild type, mutated Fep1-N238 4CS and 2CS-overproducing cells lost almost reddish color, suggesting that these mutants most likely impaired iron-binding property of Fep1 (Fig II-7). Fep1-N114 2CS-expressed cells also showed the same result. The Cys mutant proteins 4CS and 2CS (28.1 kDa with His-tag) was purified by nickel affinity agarose and confirmed on SDS-PAGE gel (Fig II-8). Absorption spectrum of the Fep1-N238 4CS mutant showed that it lost the majority of the characteristic absorption peaks, leaving only some residual absorption at 320 and 420 nm (Fig II-11). Besides 4CS mutant, 2CS mutants lost reddish brown color and the majority of the characteristic absorption peaks (Fig II-12). This indicates that the conserved cysteines are critical in binding the iron cofactor, most likely as coordinating ligands.

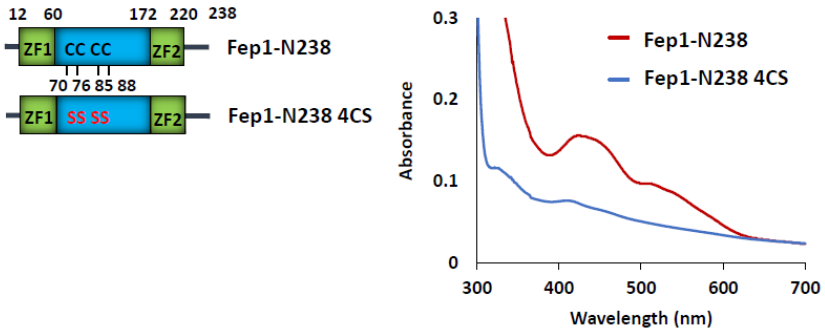

Fig II-11. UV-visible absorption spectra of aerobically purified Fep1-N238 & Fep1-N238 4CS (C70S, C76S, C85S, C88S)

UV-visible absorption spectra of Fep1-N238 with 4CS mutation (blue line) in comparison with the wild type (red)

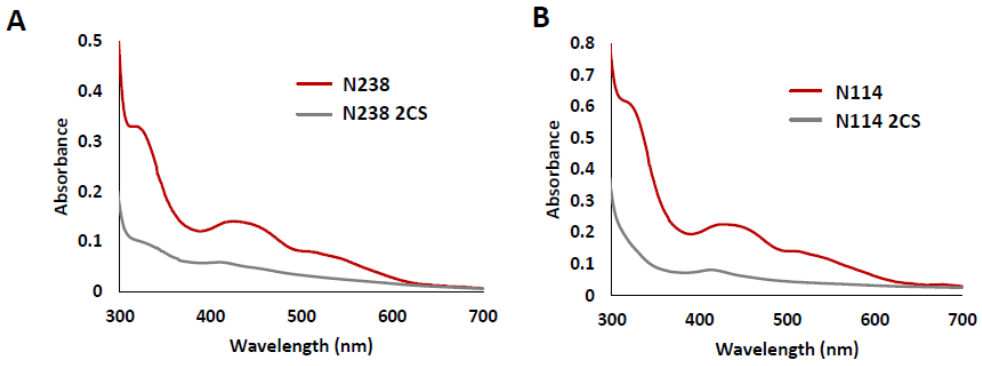

Fig II-12. UV-visible absorption spectrum of truncated Fep1 & truncated Fep1 2CS

UV-visible absorption spectra of truncated Fep1 with 2CS (C85/88S) mutation (gray line) in comparison with the wild type (red line)

III. 2.3. Both iron and sulfide are required to reconstitute iron-bound Fep1

In order to further confirm the presence of Fe-S cluster in Fep1, we prepared apo-Fep1-N238 from the purified protein and tried reconstitution of metal cofactor under anaerobic condition. The reconstitution mixture contained ferric chloride ($FeCl_3$) with or without sodium sulfide (Na_2S). Results in Fig II-13. demonstrated that the addition of sodium sulfide produced Fep1 with absorption spectrum similar to that of the as isolated Fep1. Iron alone did not produce the form with the characteristic absorption spectrum. Compared with apo-Fep1, the iron-only reconstitution resulted in increased absorption below 400 nm, suggestive of some iron binding. The degraded Fep1 fragments-containing Full-length Fep1 showed the same result (Fig II-14).

III. 2.4. Iron and acid labile sulfide content of purified Fep1-N238

I then determined the content of iron and sulfide in the anaerobically purified Fep1-N238. [2Fe-2S]-containing SoxR protein was assayed in parallel as a positive control for Fe-S detection. In my hands, as isolated SoxR was determined to contain 0.33 and 0.34 atoms of iron and sulfide, respectively, per monomeric protein (Table II-1), consistent with the presence of [2Fe-2S] cluster, even though not fully metallated. Incomplete Fe-S cluster bound to Fep1 may be limited by *E. coli* overexpression system. The apo-Fep1 protein contained 0.04 and 0.03 atoms of iron and sulfide, indicating successful de-metallation. The wild type Fep1-N238 contained 0.37 ± 0.02 atoms of iron and 0.30 ± 0.09 atoms of sulfide per monomeric protein. The roughly 1:1 ratio of iron to sulfide is indicative of the presence

of Fe-S cluster. The 4CS mutant, on the other hand, showed much lower amount of iron and sulfide (0.17 ± 0.02 iron and 0.07 ± 0.07 sulfide per monomer), consistent with the mostly bleached absorption spectrum of the mutant protein. Some residual amount of iron in the 4CS mutant suggests that there could be some weaker binding site(s) for iron, possibly in the zinc-finger domains. This coincides with the low level of absorption by 4CS mutant (Fig II-11).

The reconstituted Fep1 was determined to contain 3.14 and 3.26 atoms of iron and sulfide, respectively, per monomer (Table II-1). The nearly 1:1 ratio of iron to sulfide again supports the presence of Fe-S cluster in the reconstituted Fep1. The stoichiometry suggests the possibility of more than one [2Fe-2S], or the presence of [4Fe-4S], or a mixture of clusters. The results indicated that both iron and sulfide are required for reconstitution of the Fep1-N238. Thus, we could confirm again our conclusion that Fep1-N238 binds Fe-S clusters.

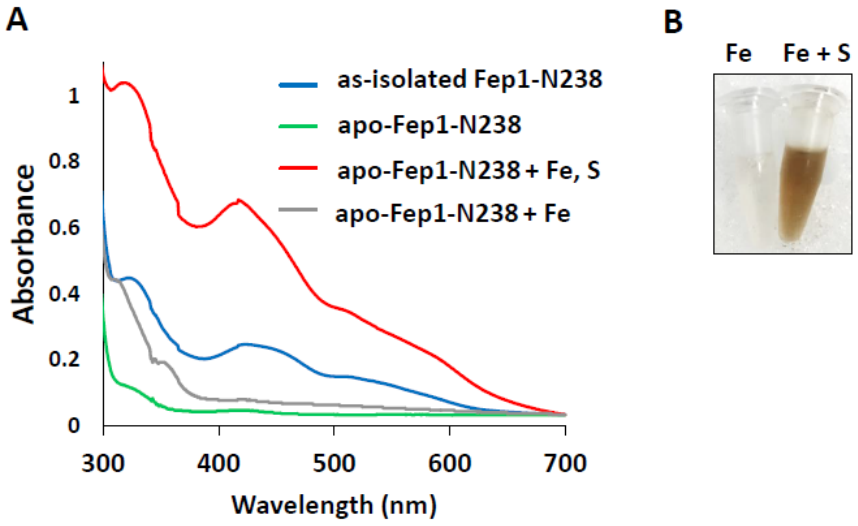

Fig II-13. Iron and sulfide requirement to reconstitute iron-bound Fep1-N238.

A. Absorption spectra were taken for purified Fep1-N238 (as isolated, blue), apo-Fep1-N238 (green), or the reconstituted one in the presence of iron and sulfide (red), or iron only (gray).

B. Reconstituted Fep1 with both Fe and Sulfide has a reddish brown color (right side) compared with only Fe addition (left side).

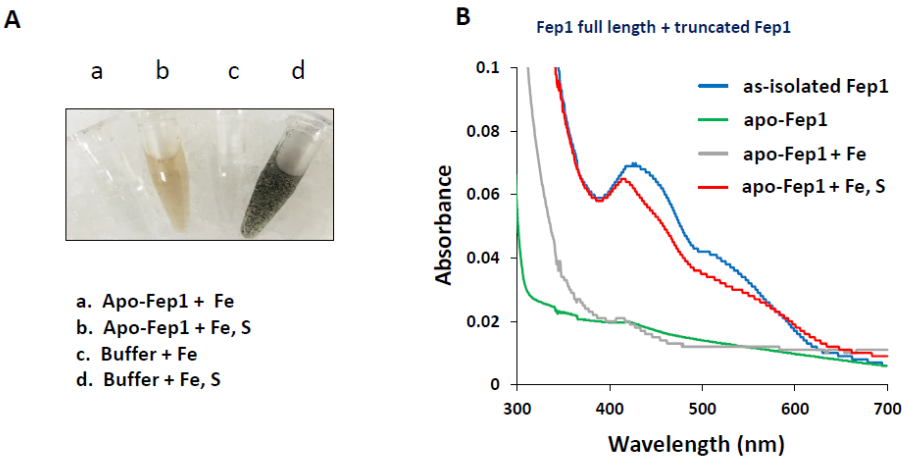

Fig II-14. Iron and sulfide requirement to reconstitute iron-bound full-length Fep1

A. Reconstituted Fep1 with both Fe and Sulfide has a reddish brown color (b) compared with only Fe addition (a).

B. Absorption spectra were taken for purified full-length and truncated Fep1 (as isolated, blue), apo-Fep1 (green), or the reconstituted one in the presence of iron and sulfide (red), or iron only (gray).

	Fep1-N238	Fep1-N238 4CS	Apo-Fep1-N238	Reconstituted Fep1-N238	SoxR (*E. coli*)
Fe/ monomer	0.37 ± 0.02	0.17 ± 0.02	0.04 ± 0.06	3.14 ± 0.94	0.33 ± 0.09
Sulfide/ monomer	0.30 ± 0.09	0.07 ± 0.07	0.03 ± 0.08	3.26 ± 0.99	0.34 ± 0.08

Table II-1. Iron and acid labile sulfide content of purified Fep1-N238

Iron concentration in the purified protein sample was determined by colorimetric ferrozine assay. Acid labile sulfide concentration was determined by using methylene blue-based color assay. The amount of iron and acid labile sulfide was determined for three independently prepared protein samples. Stoichiometry per monomeric protein was presented.

Sample	Experimental mass	Theoretical mass
Fep1	128800	62900
Fep1-N238	62900	28100
Fep1-N238 4CS	61600	28100
Apo-Fep1-N238	62600	28100
Reconstituted Fep1-N238	60100	28100

All masses are shown in Da.

Table II-2. Molecular mass analysis of Fep1

Experimental mass (shown in Da) is from gel filtration analyses.

III. 3. EPR analyses of Fep1-N238

To further obtain information on the type of Fe-S cluster in the purified (as isolated) Fep1-N238, we pursued electron paramagnetic resonance (EPR) spectroscopy. At 123 K, broad isotropic signal around a g-factor value of 2.01 was detected in the dithionite-treated (reduced) sample (Fig II-16). The peak is indicative of the presence of $[2Fe\text{-}2S]^{2+}$ cluster in the purified protein that becomes visible in EPR when reduced to paramagnetic $[2Fe\text{-}2S]^{1+}$ (spin status 1/2). The presence of oxidized status of iron in the purified Fep1 protein is reminiscent of SoxR we analyzed by EPR previously (Lee, Singh et al., 2015, Singh, Shin et al., 2013). To resolve broad isotropic signal at 123 K, we prepared another batch of Fep1-N238 samples, and performed EPR analysis with liquid helium cryostat. At 5 K, as isolated Fep1-N238 samples exhibited two different types of signal depending on sample preparation. For one sample, a single rhombic signal near a g-factor value of 4.3 was detected in the purified sample, suggesting the presence of mononuclear ferric ion (Fig II-17A). Reduction by sodium dithionite produced a signal near a g-factor value of approx. 2.00, indicative of spin status 1/2 from $[2Fe\text{-}2S]^{1+}$ or $[4Fe\text{-}4S]^{1+}$ cluster (Fig II-17A). In the third sample, two rhombic signals near g-factor values of 4.3 and 2.00 were observed in the absence of dithionite reduction, which nearly disappeared in the dithionite-treated sample (Fig II-17B). The peaks remained unchanged when oxidized by ferricyanide (data not shown). The signals observed near g-factor values of 4.3 and 2.00 under oxidized condition resemble those typically observed for a linear [3Fe-4S] cluster with spin status 5/2. Both signals decreased by elevating the temperatrure to 10 K (data not shown), supporting the

presence of linear 3Fe-4S. Taken together, the EPR analyses confirmed the presence of Fe-S cluster in the purified as isolated Fep1, and suggests the possibility of mixed population of multiple Fe-S cluster types that could involve [2Fe-2S], [3Fe-4S], [4Fe-4S], and a mononuclear iron. The diverse EPR spectra observed in different samples may reflect the versatile intracellular environment of Fe-S cluster in Fep1 that form a complex with Grx4 and Fra2. Depending on the condition of cell lysis and early steps of purification, different populations of Fe-S cluster could be captured in the purified protein samples as snapshots. Further systematic spectroscopic analyses are in need to elucidate the exact cluster type and the time course of conversion, if any.

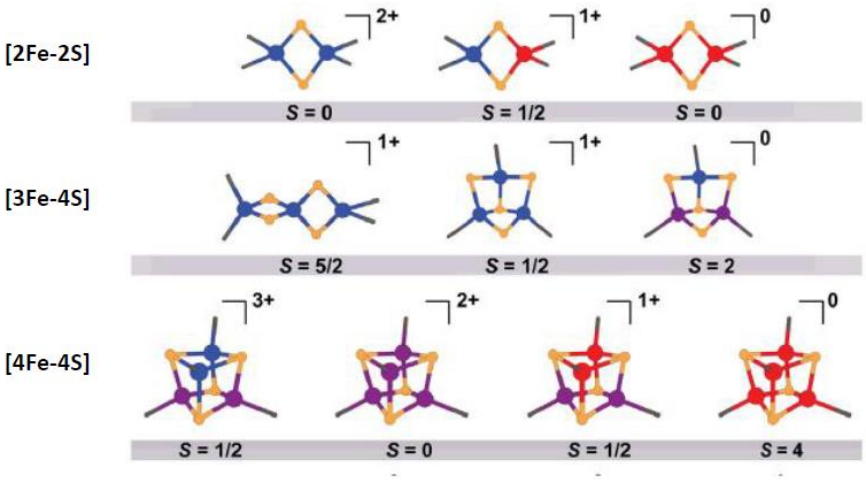

Fig II-15. Most important types of Fe-S clusters encountered in nature and their corresponding electronic properties. (Pandelia, Lanz et al., 2015)

Fe^{3+} is represented with blue, $Fe^{2+}$with red and the mixed-valent $Fe^{2.5+}$ with purple spheres. Sulfide ligands are depicted with yellow spheres.

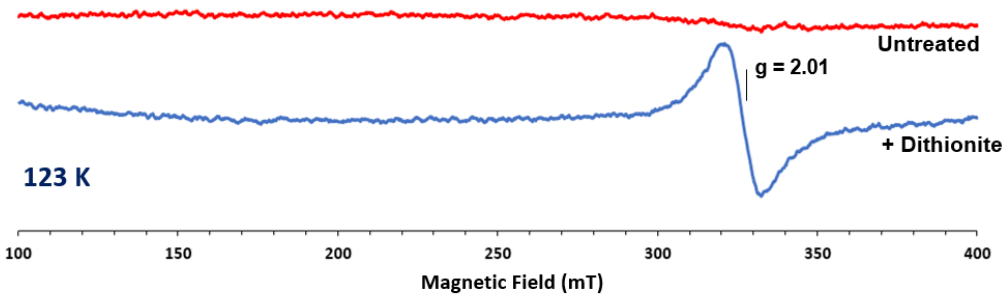

Fig II-16. EPR spectra of as-isolated Fep1-N238 analyzed at 123 K

Anaerobically purified Fep1 (*red line*) was reduced by dithionite (*blue line*), and it was transferred to EPR tubes, and incubated anaerobically for 10 min at room temperature, and immediately frozen in liquid nitrogen. Fep1-N238 protein samples were subjected to EPR analyses. Microwave power, 1 mW; Microwave frequency, 9.17 GHz; Modulation frequency, 100 KHz; Temperature, 123 K

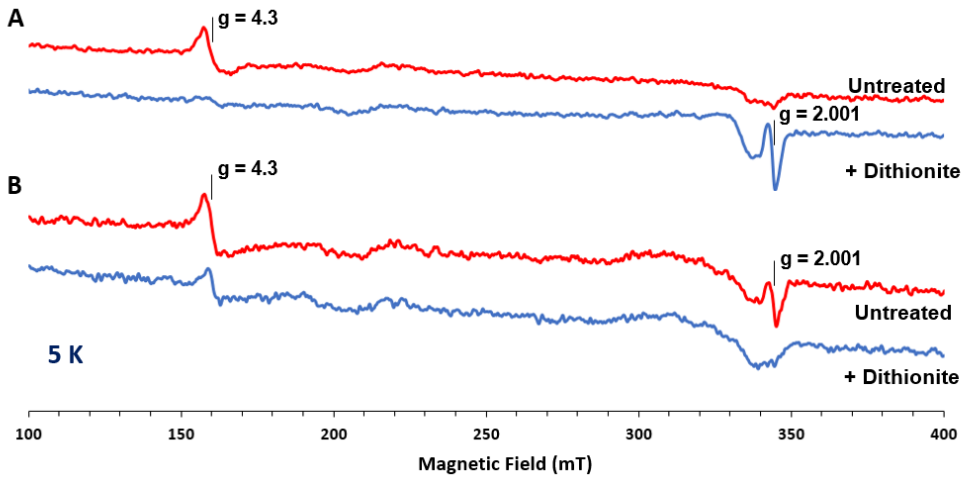

Fig II-17. EPR spectra of as-isolated Fep1-N238 analyzed at 5 K

Anaerobically purified Fep1-N238 protein samples with or without dithionite treatments were subjected to EPR analyses. The following settings were used throughout the measurement: (A),(B) Microwave power, 1 mW; Microwave frequency, 9.64 GHz; Modulation frequency, 100 kHz; Modulation Amplitude, 10 Gauss; Temperature, 5 K.

CHAPTER IV.
CONCLUSION

Recently, Hidalgo and her colleagues (Encinar del Dedo et al., 2015) reported that Fep1 is an iron-binding protein, but not an Fe-S protein, based on analysis of GST-tagged truncated Fep1. We analyzed His-tagged Fep1, and showed that both the full length and N238 fragment of Fep1 show nearly identical UV-Vis absorption spectra characteristic of Fe-S proteins. I observed 1:1 stoichiometric amounts of iron and sulfide in both reconstituted and as isolated proteins, indicative of Fe-S cluster. We took precautions for reproducible quantification of sulfide content, which can be hindered by the presence of reducing agent such as DTT or glutathione in the buffer. The absorption spectrum, quantification of iron and sulfide, metal reconstitution, and EPR analyses all support the presence of Fe-S cluster in Fep1.

Our finding that Fep1 contains Fe-S cluster fits nicely with the current model of iron signaling that involve Grx4, whose conserved cysteines in the glutaredoxin domain is required to inhibit Fep1 activity under iron starvation condition (Encinar del Dedo et al., 2015, Jbel et al., 2011, Kim et al., 2011), and the interaction of [Fe-S]-binding Grx4-Fra2 heterodimer with Fep1 (Fig II-19). Demonstration of [Fe-S] in Fep1 leads to a proposal that there could be a two-way trafficking of [Fe-S] between Grx4-Fra2 complex and Fep1. Under iron starvation condition, [Fe-S] cluster may be transferred to Grx4-Fra2, resulting in inhibition of DNA-binding activity of Fep1 and subsequent derepression of iron acquisition genes (Fig II-19). Under iron replete condition, Fep1 may acquire [Fe-S] by itself or from the [Fe-S]-bound Grx4-Fra2. The finding that iron acquisition genes remain repressed in *grx*4 mutant even under iron starved condition suggest that the [Fe-S] binding

in Fep1 is quite stable in the absence of Grx4. Whether a two-way transfer of [Fe-S] between Fep1 and Grx4-Fra2 complex occurs *in vitro* and *in vivo* needs be elucidated in the future. In both prokaryotes and eukaryotes, CGFS-type monothiol glutaredoxins are known to incorporate [2Fe-2S] cluster (Picciocchi et al., 2007). The exact type of Fe-S cluster in Grx4 of *S. pombe* has not been determined experimentally, even though it is likely to be [2Fe-2S] as observed in *S. cerevisiae*. Future studies on the transfer of Fe-S cluster between Fep1 and Grx4-Fra2 complex (Fig II-20) will reveal a key mechanism behind the iron-regulation of Fep1 activity. Whether Fep1 orthologs in other fungi bind [Fe-S] and utilize monothiol glutaredoxin to convey iron signaling via cluster transfer will be another interesting subject to investigate.

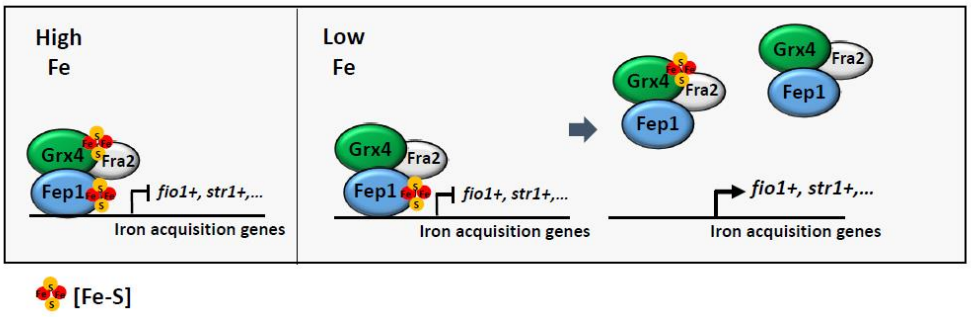

Fig II-19. A proposed model of iron-dependent regulation of Fep1 repressor activity

Under iron-replete conditions, Grx4-Fra2 heterodimer might acquire an [2Fe-2S] cluster. Fep1 also binds an [Fe-S] cluster and can represses expression of iron acquisition genes. Intracellular Fe depletion could trigger Fe loss from the Fe-S cluster bridging Grx4 and Fra2 first, the heterodimer can then [Fe-S] cluster from Fep1, which would then become inactive as a transcriptional repressor.

Protein-protein interaction studies have revealed that Grx4 interacts Fep1 and Fra2 iron-independently. Fep1 also interacts Fra2 iron-independently (J.F. Jacques *et al*., 2014, J. Encinar *et al*., 2015, K.D Kim *et al*.,2011).

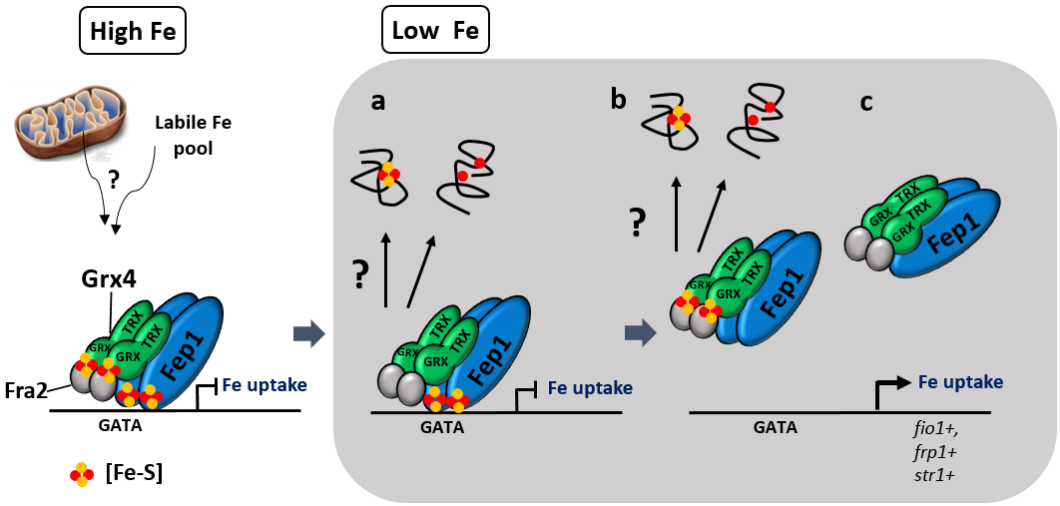

Fig II-20. A proposed model of iron-dependent regulation of Fep1 repressor activity

Under iron-replete conditions, Grx4-Fra2 heterodimer might acquire an [2Fe-2S] cluster. Fep1 also binds an [Fe-S] cluster and can represses expression of iron acquisition genes. Intracellular Fe depletion could trigger Fe loss from the Fe-S cluster bridging Grx4 and Fra2 first (a), the heterodimer can then [Fe-S] cluster from Fep1, which would then become inactive as a transcriptional repressor (b).

Protein-protein interaction studies have revealed that Grx4 interacts Fep1 and Fra2 iron-independently. Fep1 also interacts Fra2 iron-independently (J.F. Jacques *et al.*, 2014, J. Encinar *et al.*, 2015, K.D Kim *et al.*,2011).

The Trx-like domain (TRX) of Grx4 interacts with the C-terminal region of Fep1 iron-independently, whereas the Grx-like domain (GRX) of Grx4 weakly interacts with the N-terminal region of Fep1 only under low iron condition (c) (M. Jbel *et al.*, 2011).

REFERENCES

Alves R, Herrero E, Sorribas A (2004) Predictive reconstruction of the mitochondrial iron-sulfur cluster assembly metabolism. II. Role of glutaredoxin Grx5. Proteins 57: 481-92

An Z, Mei B, Yuan WM, Leong SA (1997) The distal GATA sequences of the sid1 promoter of Ustilago maydis mediate iron repression of siderophore production and interact directly with Urbs1, a GATA family transcription factor. EMBO J 16: 1742-50

Arabidopsis Interactome Mapping C (2011) Evidence for network evolution in an Arabidopsis interactome map. Science 333: 601-7

Askwith C, Kaplan J (1998) Iron and copper transport in yeast and its relevance to human disease. Trends Biochem Sci 23: 135-8

Babichev Y, Isakov N (2001) Tyrosine phosphorylation of PICOT and its translocation to the nucleus in response of human T cells to oxidative stress. Adv Exp Med Biol 495: 41-5

Bandyopadhyay S, Gama F, Molina-Navarro MM, Gualberto JM, Claxton R, Naik SG, Huynh BH, Herrero E, Jacquot JP, Johnson MK, Rouhier N (2008) Chloroplast monothiol glutaredoxins as scaffold proteins for the assembly and delivery of [2Fe-2S] clusters. EMBO J 27: 1122-33

Beinert H (1983) Semi-micro methods for analysis of labile sulfide and of labile sulfide plus sulfane sulfur in unusually stable iron-sulfur proteins. Anal Biochem 131: 373-8

Belli G, Polaina J, Tamarit J, De La Torre MA, Rodriguez-Manzaneque MT, Ros J, Herrero E (2002) Structure-function analysis of yeast Grx5 monothiol glutaredoxin defines essential amino acids for the function of the protein. J Biol Chem 277: 37590-6

Bleackley MR, Macgillivray RT (2011) Transition metal homeostasis: from yeast to human disease. Biometals 24: 785-809

Brault A, Mourer T, Labbe S (2015) Molecular basis of the regulation of iron homeostasis in fission and filamentous yeasts. IUBMB Life 67: 801-15

Butland G, Babu M, Diaz-Mejia JJ, Bohdana F, Phanse S, Gold B, Yang W, Li J, Gagarinova AG, Pogoutse O, Mori H, Wanner BL, Lo H, Wasniewski J, Christopolous C, Ali M, Venn P, Safavi-Naini A, Sourour N, Caron S et al. (2008) eSGA: E. coli synthetic genetic array analysis. Nat Methods 5: 789-95

Chao LY, Marletta MA, Rine J (2008) Sre1, an iron-modulated GATA DNA-binding protein of iron-uptake genes in the fungal pathogen Histoplasma capsulatum. Biochemistry 47: 7274-83

Cheng NH, Liu JZ, Liu X, Wu Q, Thompson SM, Lin J, Chang J, Whitham SA, Park

S, Cohen JD, Hirschi KD (2011) Arabidopsis monothiol glutaredoxin, AtGRXS17, is critical for temperature-dependent postembryonic growth and development via modulating auxin response. J Biol Chem 286: 20398-406
Cheng NH, Zhang W, Chen WQ, Jin J, Cui X, Butte NF, Chan L, Hirschi KD (2011) A mammalian monothiol glutaredoxin, Grx3, is critical for cell cycle progression during embryogenesis. FEBS J 278: 2525-39
Couturier J, Jacquot JP, Rouhier N (2009) Evolution and diversity of glutaredoxins in photosynthetic organisms. Cell Mol Life Sci 66: 2539-57
Couturier J, Wu HC, Dhalleine T, Pegeot H, Sudre D, Gualberto JM, Jacquot JP, Gaymard F, Vignols F, Rouhier N (2014) Monothiol glutaredoxin-BolA interactions: redox control of Arabidopsis thaliana BolA2 and SufE1. Mol Plant 7: 187-205
De Freitas J, Wintz H, Kim JH, Poynton H, Fox T, Vulpe C (2003) Yeast, a model organism for iron and copper metabolism studies. Biometals 16: 185-97
Dhalleine T, Rouhier N, Couturier J (2014) Putative roles of glutaredoxin-BolA holo-heterodimers in plants. Plant Signal Behav 9: e28564
Encinar del Dedo J, Gabrielli N, Carmona M, Ayte J, Hidalgo E (2015) A cascade of iron-containing proteins governs the genetic iron starvation response to promote iron uptake and inhibit iron storage in fission yeast. PLoS Genet 11: e1005106
Fernandes AP, Fladvad M, Berndt C, Andresen C, Lillig CH, Neubauer P, Sunnerhagen M, Holmgren A, Vlamis-Gardikas A (2005) A novel monothiol glutaredoxin (Grx4) from Escherichia coli can serve as a substrate for thioredoxin reductase. J Biol Chem 280: 24544-52
Fernandes AP, Holmgren A (2004) Glutaredoxins: glutathione-dependent redox enzymes with functions far beyond a simple thioredoxin backup system. Antioxid Redox Signal 6: 63-74
Fleming RE, Ponka P (2012) Iron overload in human disease. N Engl J Med 366: 348-59
Giot L, Bader JS, Brouwer C, Chaudhuri A, Kuang B, Li Y, Hao YL, Ooi CE, Godwin B, Vitols E, Vijayadamodar G, Pochart P, Machineni H, Welsh M, Kong Y, Zerhusen B, Malcolm R, Varrone Z, Collis A, Minto M et al. (2003) A protein interaction map of Drosophila melanogaster. Science 302: 1727-36
Haas H, Zadra I, Stoffler G, Angermayr K (1999) The Aspergillus nidulans GATA factor SREA is involved in regulation of siderophore biosynthesis and control of iron uptake. J Biol Chem 274: 4613-9
Harrison KA, Marzluf GA (2002) Characterization of DNA binding and the cysteine rich region of SRE, a GATA factor in Neurospora crassa involved in siderophore synthesis. Biochemistry 41: 15288-95
Haunhorst P, Berndt C, Eitner S, Godoy JR, Lillig CH (2010) Characterization of the human monothiol glutaredoxin 3 (PICOT) as iron-sulfur protein. Biochem Biophys Res Commun 394: 372-6

Herrero E, Belli G, Casa C (2010) Structural and functional diversity of glutaredoxins in yeast. Curr Protein Pept Sci 11: 659-68
Ho Y, Gruhler A, Heilbut A, Bader GD, Moore L, Adams SL, Millar A, Taylor P, Bennett K, Boutilier K, Yang L, Wolting C, Donaldson I, Schandorff S, Shewnarane J, Vo M, Taggart J, Goudreault M, Muskat B, Alfarano C et al. (2002) Systematic identification of protein complexes in Saccharomyces cerevisiae by mass spectrometry. Nature 415: 180-3
Hoffmann B, Uzarska MA, Berndt C, Godoy JR, Haunhorst P, Lillig CH, Lill R, Muhlenhoff U (2011) The multidomain thioredoxin-monothiol glutaredoxins represent a distinct functional group. Antioxid Redox Signal 15: 19-30
Hu CD, Chinenov Y, Kerppola TK (2002) Visualization of interactions among bZIP and Rel family proteins in living cells using bimolecular fluorescence complementation. Mol Cell 9: 789-98
Huynen MA, Spronk CA, Gabaldon T, Snel B (2005) Combining data from genomes, Y2H and 3D structure indicates that BolA is a reductase interacting with a glutaredoxin. FEBS Lett 579: 591-6
Ito T, Tashiro K, Muta S, Ozawa R, Chiba T, Nishizawa M, Yamamoto K, Kuhara S, Sakaki Y (2000) Toward a protein-protein interaction map of the budding yeast: A comprehensive system to examine two-hybrid interactions in all possible combinations between the yeast proteins. Proc Natl Acad Sci U S A 97: 1143-7
Iwema T, Picciocchi A, Traore DA, Ferrer JL, Chauvat F, Jacquamet L (2009) Structural basis for delivery of the intact [Fe2S2] cluster by monothiol glutaredoxin. Biochemistry 48: 6041-3
Jacques JF, Mercier A, Brault A, Mourer T, Labbe S (2014) Fra2 is a co-regulator of Fep1 inhibition in response to iron starvation. PLoS One 9: e98959
Jbel M, Mercier A, Labbe S (2011) Grx4 monothiol glutaredoxin is required for iron limitation-dependent inhibition of Fep1. Eukaryot Cell 10: 629-45
Jbel M, Mercier A, Pelletier B, Beaudoin J, Labbe S (2009) Iron activates in vivo DNA binding of Schizosaccharomyces pombe transcription factor Fep1 through its amino-terminal region. Eukaryot Cell 8: 649-64
Jo WJ, Loguinov A, Chang M, Wintz H, Nislow C, Arkin AP, Giaever G, Vulpe CD (2008) Identification of genes involved in the toxic response of Saccharomyces cerevisiae against iron and copper overload by parallel analysis of deletion mutants. Toxicol Sci 101: 140-51
Jung WH, Sham A, White R, Kronstad JW (2006) Iron regulation of the major virulence factors in the AIDS-associated pathogen Cryptococcus neoformans. PLoS Biol 4: e410
Kaplan J, Ward DM (2013) The essential nature of iron usage and regulation. Curr Biol 23: R642-6
Ken CF, Chen IJ, Lin CT, Liu SM, Wen L, Lin CT (2011) Monothiol glutaredoxin cDNA from Taiwanofungus camphorata: a novel CGFS-type glutaredoxin

possessing glutathione reductase activity. J Agric Food Chem 59: 3828-35
Kim KD, Chung WH, Kim HJ, Lee KC, Roe JH (2010) Monothiol glutaredoxin Grx5 interacts with Fe-S scaffold proteins Isa1 and Isa2 and supports Fe-S assembly and DNA integrity in mitochondria of fission yeast. Biochemical and biophysical research communications 392: 467-72
Kim KD, Kim HJ, Lee KC, Roe JH (2011) Multi-domain CGFS-type glutaredoxin Grx4 regulates iron homeostasis via direct interaction with a repressor Fep1 in fission yeast. Biochem Biophys Res Commun 408: 609-14
Krogan NJ, Cagney G, Yu H, Zhong G, Guo X, Ignatchenko A, Li J, Pu S, Datta N, Tikuisis AP, Punna T, Peregrin-Alvarez JM, Shales M, Zhang X, Davey M, Robinson MD, Paccanaro A, Bray JE, Sheung A, Beattie B et al. (2006) Global landscape of protein complexes in the yeast Saccharomyces cerevisiae. Nature 440: 637-43
Kumanovics A, Chen OS, Li L, Bagley D, Adkins EM, Lin H, Dingra NN, Outten CE, Keller G, Winge D, Ward DM, Kaplan J (2008) Identification of FRA1 and FRA2 as genes involved in regulating the yeast iron regulon in response to decreased mitochondrial iron-sulfur cluster synthesis. J Biol Chem 283: 10276-86
Labbe S, Khan MG, Jacques JF (2013) Iron uptake and regulation in Schizosaccharomyces pombe. Curr Opin Microbiol 16: 669-76
Lan CY, Rodarte G, Murillo LA, Jones T, Davis RW, Dungan J, Newport G, Agabian N (2004) Regulatory networks affected by iron availability in Candida albicans. Mol Microbiol 53: 1451-69
Lee KL, Singh AK, Heo L, Seok C, Roe JH (2015) Factors affecting redox potential and differential sensitivity of SoxR to redox-active compounds. Mol Microbiol 97: 808-21
Li H, Mapolelo DT, Dingra NN, Keller G, Riggs-Gelasco PJ, Winge DR, Johnson MK, Outten CE (2011) Histidine 103 in Fra2 is an iron-sulfur cluster ligand in the [2Fe-2S] Fra2-Grx3 complex and is required for in vivo iron signaling in yeast. J Biol Chem 286: 867-76
Li H, Mapolelo DT, Dingra NN, Naik SG, Lees NS, Hoffman BM, Riggs-Gelasco PJ, Huynh BH, Johnson MK, Outten CE (2009) The yeast iron regulatory proteins Grx3/4 and Fra2 form heterodimeric complexes containing a [2Fe-2S] cluster with cysteinyl and histidyl ligation. Biochemistry 48: 9569-81
Li H, Mapolelo DT, Randeniya S, Johnson MK, Outten CE (2012) Human glutaredoxin 3 forms [2Fe-2S]-bridged complexes with human BolA2. Biochemistry 51: 1687-96
Lill R, Muhlenhoff U (2008) Maturation of iron-sulfur proteins in eukaryotes: mechanisms, connected processes, and diseases. Annu Rev Biochem 77: 669-700
Lillig CH, Berndt C, Holmgren A (2008) Glutaredoxin systems. Biochim Biophys Acta 1780: 1304-17
Lin H, Li L, Jia X, Ward DM, Kaplan J (2011) Genetic and biochemical analysis of

high iron toxicity in yeast: iron toxicity is due to the accumulation of cytosolic iron and occurs under both aerobic and anaerobic conditions. J Biol Chem 286: 3851-62
Lodi R, Tonon C, Calabrese V, Schapira AH (2006) Friedreich's ataxia: from disease mechanisms to therapeutic interventions. Antioxid Redox Signal 8: 438-43
Lopreiato R, Facchin S, Sartori G, Arrigoni G, Casonato S, Ruzzene M, Pinna LA, Carignani G (2004) Analysis of the interaction between piD261/Bud32, an evolutionarily conserved protein kinase of Saccharomyces cerevisiae, and the Grx4 glutaredoxin. Biochem J 377: 395-405
Mercier A, Labbe S (2009) Both Php4 function and subcellular localization are regulated by iron via a multistep mechanism involving the glutaredoxin Grx4 and the exportin Crm1. J Biol Chem 284: 20249-62
Mercier A, Pelletier B, Labbe S (2006) A transcription factor cascade involving Fep1 and the CCAAT-binding factor Php4 regulates gene expression in response to iron deficiency in the fission yeast Schizosaccharomyces pombe. Eukaryot Cell 5: 1866-81
Mercier A, Watt S, Bahler J, Labbe S (2008) Key function for the CCAAT-binding factor Php4 to regulate gene expression in response to iron deficiency in fission yeast. Eukaryot Cell 7: 493-508
Mesecke N, Mittler S, Eckers E, Herrmann JM, Deponte M (2008) Two novel monothiol glutaredoxins from Saccharomyces cerevisiae provide further insight into iron-sulfur cluster binding, oligomerization, and enzymatic activity of glutaredoxins. Biochemistry 47: 1452-63
Molina-Navarro MM, Casas C, Piedrafita L, Belli G, Herrero E (2006) Prokaryotic and eukaryotic monothiol glutaredoxins are able to perform the functions of Grx5 in the biogenesis of Fe/S clusters in yeast mitochondria. FEBS Lett 580: 2273-80
Molina MM, Belli G, de la Torre MA, Rodriguez-Manzaneque MT, Herrero E (2004) Nuclear monothiol glutaredoxins of Saccharomyces cerevisiae can function as mitochondrial glutaredoxins. J Biol Chem 279: 51923-30
Moreno S, Klar A, Nurse P (1991) Molecular genetic analysis of fission yeast Schizosaccharomyces pombe. Methods Enzymol 194: 795-823
Muhlenhoff U, Gerber J, Richhardt N, Lill R (2003) Components involved in assembly and dislocation of iron-sulfur clusters on the scaffold protein Isu1p. EMBO J 22: 4815-25
Muhlenhoff U, Molik S, Godoy JR, Uzarska MA, Richter N, Seubert A, Zhang Y, Stubbe J, Pierrel F, Herrero E, Lillig CH, Lill R (2010) Cytosolic monothiol glutaredoxins function in intracellular iron sensing and trafficking via their bound iron-sulfur cluster. Cell Metab 12: 373-85
Nairz M, Weiss G (2006) Molecular and clinical aspects of iron homeostasis: From anemia to hemochromatosis. Wien Klin Wochenschr 118: 442-62
Ojeda L, Keller G, Muhlenhoff U, Rutherford JC, Lill R, Winge DR (2006) Role of glutaredoxin-3 and glutaredoxin-4 in the iron regulation of the Aft1 transcriptional

activator in Saccharomyces cerevisiae. J Biol Chem 281: 17661-9
Pandelia ME, Lanz ND, Booker SJ, Krebs C (2015) Mossbauer spectroscopy of Fe/S proteins. Biochim Biophys Acta 1853: 1395-405
Pandolfo M, Pastore A (2009) The pathogenesis of Friedreich ataxia and the structure and function of frataxin. J Neurol 256 Suppl 1: 9-17
Pelletier B, Beaudoin J, Philpott CC, Labbe S (2003) Fep1 represses expression of the fission yeast Schizosaccharomyces pombe siderophore-iron transport system. Nucleic Acids Res 31: 4332-44
Pelletier B, Trott A, Morano KA, Labbe S (2005) Functional characterization of the iron-regulatory transcription factor Fep1 from Schizosaccharomyces pombe. J Biol Chem 280: 25146-61
Philpott CC, Leidgens S, Frey AG (2012) Metabolic remodeling in iron-deficient fungi. Biochim Biophys Acta 1823: 1509-20
Picciocchi A, Saguez C, Boussac A, Cassier-Chauvat C, Chauvat F (2007) CGFS-type monothiol glutaredoxins from the cyanobacterium Synechocystis PCC6803 and other evolutionary distant model organisms possess a glutathione-ligated [2Fe-2S] cluster. Biochemistry 46: 15018-26
Poor CB, Wegner SV, Li H, Dlouhy AC, Schuermann JP, Sanishvili R, Hinshaw JR, Riggs-Gelasco PJ, Outten CE, He C (2014) Molecular mechanism and structure of the Saccharomyces cerevisiae iron regulator Aft2. Proc Natl Acad Sci U S A 111: 4043-8
Pujol-Carrion N, Belli G, Herrero E, Nogues A, de la Torre-Ruiz MA (2006) Glutaredoxins Grx3 and Grx4 regulate nuclear localisation of Aft1 and the oxidative stress response in Saccharomyces cerevisiae. J Cell Sci 119: 4554-64
Pujol-Carrion N, de la Torre-Ruiz MA (2010) Glutaredoxins Grx4 and Grx3 of Saccharomyces cerevisiae play a role in actin dynamics through their Trx domains, which contributes to oxidative stress resistance. Appl Environ Microbiol 76: 7826-35
Riemer J, Hoepken HH, Czerwinska H, Robinson SR, Dringen R (2004) Colorimetric ferrozine-based assay for the quantitation of iron in cultured cells. Anal Biochem 331: 370-5
Rodriguez-Manzaneque MT, Ros J, Cabiscol E, Sorribas A, Herrero E (1999) Grx5 glutaredoxin plays a central role in protection against protein oxidative damage in Saccharomyces cerevisiae. Mol Cell Biol 19: 8180-90
Rodriguez-Manzaneque MT, Tamarit J, Belli G, Ros J, Herrero E (2002) Grx5 is a mitochondrial glutaredoxin required for the activity of iron/sulfur enzymes. Mol Biol Cell 13: 1109-21
Rouault TA, Tong WH (2008) Iron-sulfur cluster biogenesis and human disease. Trends Genet 24: 398-407
Rouhier N, Couturier J, Johnson MK, Jacquot JP (2010) Glutaredoxins: roles in iron homeostasis. Trends Biochem Sci 35: 43-52

Rouhier N, Unno H, Bandyopadhyay S, Masip L, Kim SK, Hirasawa M, Gualberto JM, Lattard V, Kusunoki M, Knaff DB, Georgiou G, Hase T, Johnson MK, Jacquot JP (2007) Functional, structural, and spectroscopic characterization of a glutathione-ligated [2Fe-2S] cluster in poplar glutaredoxin C1. Proc Natl Acad Sci U S A 104: 7379-84
Rutherford JC, Ojeda L, Balk J, Muhlenhoff U, Lill R, Winge DR (2005) Activation of the iron regulon by the yeast Aft1/Aft2 transcription factors depends on mitochondrial but not cytosolic iron-sulfur protein biogenesis. J Biol Chem 280: 10135-40
Schrettl M, Kim HS, Eisendle M, Kragl C, Nierman WC, Heinekamp T, Werner ER, Jacobsen I, Illmer P, Yi H, Brakhage AA, Haas H (2008) SreA-mediated iron regulation in Aspergillus fumigatus. Mol Microbiol 70: 27-43
Sheftel A, Stehling O, Lill R (2010) Iron-sulfur proteins in health and disease. Trends Endocrinol Metab 21: 302-14
Singh AK, Shin JH, Lee KL, Imlay JA, Roe JH (2013) Comparative study of SoxR activation by redox-active compounds. Mol Microbiol 90: 983-96
Sipiczki (1989) Taxonomy and phylogenesis. In molecular biology of the fission yeast. Academic Press, London: 431-452
Sung MK, Huh WK (2007) Bimolecular fluorescence complementation analysis system for in vivo detection of protein-protein interaction in Saccharomyces cerevisiae. Yeast 24: 767-75
Tamarit J, Belli G, Cabiscol E, Herrero E, Ros J (2003) Biochemical characterization of yeast mitochondrial Grx5 monothiol glutaredoxin. J Biol Chem 278: 25745-51
Ueta R, Fujiwara N, Iwai K, Yamaguchi-Iwai Y (2012) Iron-induced dissociation of the Aft1p transcriptional regulator from target gene promoters is an initial event in iron-dependent gene suppression. Mol Cell Biol 32: 4998-5008
Vachon P, Mercier A, Jbel M, Labbe S (2012) The monothiol glutaredoxin Grx4 exerts an iron-dependent inhibitory effect on Php4 function. Eukaryot Cell 11: 806-19
Vilella F, Alves R, Rodriguez-Manzaneque MT, Belli G, Swaminathan S, Sunnerhagen P, Herrero E (2004) Evolution and cellular function of monothiol glutaredoxins: involvement in iron-sulphur cluster assembly. Comp Funct Genomics 5: 328-41
Wingert RA, Galloway JL, Barut B, Foott H, Fraenkel P, Axe JL, Weber GJ, Dooley K, Davidson AJ, Schmid B, Paw BH, Shaw GC, Kingsley P, Palis J, Schubert H, Chen O, Kaplan J, Zon LI, Tubingen Screen C (2005) Deficiency of glutaredoxin 5 reveals Fe-S clusters are required for vertebrate haem synthesis. Nature 436: 1035-39
Wood V, Gwilliam R, Rajandream MA, Lyne M, Lyne R, Stewart A, Sgouros J, Peat N, Hayles J, Baker S, Basham D, Bowman S, Brooks K, Brown D, Brown S, Chillingworth T, Churcher C, Collins M, Connor R, Cronin A et al. (2002) The

genome sequence of Schizosaccharomyces pombe. Nature 415: 871-80
Ye H, Jeong SY, Ghosh MC, Kovtunovych G, Silvestri L, Ortillo D, Uchida N, Tisdale J, Camaschella C, Rouault TA (2010) Glutaredoxin 5 deficiency causes sideroblastic anemia by specifically impairing heme biosynthesis and depleting cytosolic iron in human erythroblasts. J Clin Invest 120: 1749-61
Ye H, Rouault TA (2010) Human iron-sulfur cluster assembly, cellular iron homeostasis, and disease. Biochemistry 49: 4945-56
Yeung N, Gold B, Liu NL, Prathapam R, Sterling HJ, Willams ER, Butland G (2011) The E. coli monothiol glutaredoxin GrxD forms homodimeric and heterodimeric FeS cluster containing complexes. Biochemistry 50: 8957-69
Zaffagnini M, Michelet L, Massot V, Trost P, Lemaire SD (2008) Biochemical characterization of glutaredoxins from Chlamydomonas reinhardtii reveals the unique properties of a chloroplastic CGFS-type glutaredoxin. J Biol Chem 283: 8868-76
Zhang Y, Liu L, Wu X, An X, Stubbe J, Huang M (2011) Investigation of in vivo diferric tyrosyl radical formation in Saccharomyces cerevisiae Rnr2 protein: requirement of Rnr4 and contribution of Grx3/4 AND Dre2 proteins. J Biol Chem 286: 41499-509
Zhou LW, Haas H, Marzluf GA (1998) Isolation and characterization of a new gene, sre, which encodes a GATA-type regulatory protein that controls iron transport in Neurospora crassa. Mol Gen Genet 259: 532-40
Zimmermann MB, Hurrell RF (2007) Nutritional iron deficiency. Lancet 370: 511-20
Znaidi S, Pelletier B, Mukai Y, Labbe S (2004) The Schizosaccharomyces pombe corepressor Tup11 interacts with the iron-responsive transcription factor Fep1. J Biol Chem 279: 9462-74

국문초록

철은 세포 내에서 호흡이나, TCA cycle, DNA 복제와 수리 같은 다양한 과정에 필수적인 단백질 보조인자이다. 철은 3가 이온 (Fe3+)과 2가 이온 (Fe2+) 사이를 스위치하는 산화-환원 성질 때문에 활성 산소족을 발생시킬 수 있어 잠재적인 독성을 갖는다. 따라서 세포는 적절한 농도의 철을 유지하기 위해 엄격히 조절된다.

분열성 효모인 *Schizosaccharomyces pombe*는 두 개의 억제 전사인자에 의해 철 항상성이 조절된다. Fep1은 철 획득관련 유전자의 발현을 조절하고 Php4는 철 이용과 철 저장에 관련된 유전자의 발현을 조절하는 억제 전사인자이다. Fep1은 GATA 타입의 억제 전사인자로써 *fio1+, frp1+, str1+, str2+, str3+* 같은 철 흡수 유전자와 *abc3+*같은 액포 수송 유전자의 프로모터에 결합한다. 이로써 철이 충분한 조건일 때 세포내로 더 이상의 철 유입을 막을 수 있다.

본 실험실의 이전 연구에서 CGFS 타입의 monothiol 글루타리독신인 Grx4 결손 균주의 경우, 철 흡수와 철 이용에 관여하는 유전자의 조절이 무너진 것을 보았다. Grx4는 Fep1과 직접적으로 결합함으로써 Fep1의 활성을 조절하는데 Grx4가 필요하다는 것을 밝혀내었다. Fep1뿐 만 아니라 Php4의 경우에도 글루타리독신 Grx4에 의해서 번역 후 조절된다. 철이 충분한 조건일 경우, Grx4는 Php4와 결합하여 Php4를 세포질에 위치하도록 조절함으로써 철 이용, 저장 유전자의 발현이 증가한다. CGFS 타입의 monothiol 글루타리독신인 Grx4는 homodimer로써 Fe-S cluster를 결합한다. 혹은 BolA 타입 단백질인 Fra2와 heterodimer를 이루면서 Fe-S cluster를 갖는다고 *Saccharomyces cerevisiae*에서 알려져 있다. *S. pombe* 에서, 철이 부족한 환경일 때 Grx4와 Fra2 heterodimer가 Fep1의 DNA 결합 활성을 저해하면서 철 흡수 유전자의 발현을 증가시키는 데에 필요하다는 것이 알려져 있다.

지금까지 Fep1의 기능과 상호작용하는 단백질 파트너들이 밝혀져 왔지만, 철이 부족한 조건일 때 Fep1이 비활성화되는 분자적 기작은 아직 모른다. 본 연구에서 Fep1에 의한 철 감지 기작을 밝히기 위해 생화학적, 그리고 분광학적으로 Fep1을 분석하였다. 완전한 길이의 Fep1과 잘려진 Fep1 단백질, 그리고 *E. coli*에서 분리한 후의 자연적인 Fep1과 재구성한 Fep1에서 철과 황을 가지고 있음을 확인하였다. UV-visible spectroscopy 분석 결과 Fep1 단백질은 Fe보다는 Fe-S cluster를 결합할 것이라고 보였는데, 실제로 단백질의 철과 황을 정량 분석한 결과 약 1 : 1 의 비율로 철과 황이 검출되었다. 혐기적 조건에서 Fe과 Sulfide를 첨가하여 cluster를 재구성한 경우에도 Fep1 단백질이 갖는 Fe과 sulfide가 비슷한 비율임을 확인하였다. 또한 Fe과 Sulfide를 제공하여 재구성한 후 UV-visible spectroscopy 분석을 했을 때, Fe뿐 만 아니라 sulfide도 함께 제공해야만 본래의 Fep1이 갖는 흡광도의 특징을 볼 수 있었다. 이를 통해서 Fep1은 Fe-S cluster를 갖는 단백질임을 밝혀내었다. 또한 뮤테이션 연구를 통해 Fep1의 DNA 결합 도메인에 있는 두 zinc finger 사이의 보존된 시스테인들이 [Fe-S] 클러스터 결합에 중요함을 알게 되었다. EPR spectroscopy 분석결과 Fep1이 [2Fe-2S], [3Fe-4S], [4Fe-4S]의 여러 클러스터 타입이 혼재된 [Fe-S] 특유의 peak을 확인하였다. 본 연구결과를 통해 [Fe-S]를 갖는 monothiol Grx4가 Fep1의 활성을 조절한다는 기존 연구 결과를 더 잘 이해할 수 있다. 또한 본 연구결과는 Grx4가 Fep1의 활성을 조절하는 기작을 밝히기 위한 기반이 되어 준다.

주요 단어

Monothiol 글루타레독신, 철 항상성, Fe-S 클러스터, Fep1, *Schizosaccharomyces pombe,* EPR